Passive RF Localization Based on RSSI Using Non-linear Bayesian Estimation

A thesis submitted in partial fulfillment of the requirements for the degree of Master of Science at George Mason University

By

Anoop Kumar Palvai
Bachelor of Technology
Jawaharlal Nehru Technological University, 2005

Director: Dr. Bijan Jabbari, Professor
Department of Electrical Engineering

Fall Semester 2008
George Mason University
Fairfax, VA

DEDICATION

This work is dedicated to my parents, brothers Arun and Ajay.

ACKNOWLEDGEMENTS

It is my pleasure to thank the people who have supported me all the time.

First and foremost, I thank my thesis advisor Dr. Bijan Jabbari for providing me this opportunity. His guidance in my research is invaluable, without which, this work would not have been possible. I would also like to thank Dr. Brian Mark and Dr. Rao Mulpuri for their invaluable time.

I would like to thank my teachers especially Mr. Venkata Giri from high school and Mr. Sudhakar from undergraduate college, who instilled interest in me about engineering and mathematics.

I gratefully thank my relatives who have supported me and my family through difficult times and special thanks go to my uncle Mr. Venkat Reddy who made my M.S plans, come true.

Last but not the least, I wish to thank my parents Neeraja Palvai and Ashok Reddy Palvai for their sacrifices and guidance to make my future bright. Also I wish to thank my brothers Arun and Ajay for being a constant source of inspiration for me.

TABLE OF CONTENTS

LIST OF FIGURES

ABSTRACT

PASSIVE RF LOCALIZATION BASED ON RSSI USING NON-LINEAR BAYESIAN ESTIMATION

Anoop Kumar Palvai, MS

George Mason University, 2008

Thesis Director: Dr. Bijan Jabbari

RF localization has gained prominence because of its potential for supporting various position based applications. Passive RF Localization based on Received Signal Strength Indicator (RSSI) uses the strength of received signal from a target by passive listening to infer the range, which is subsequently used for position estimation. The thesis undertakes a study of localization techniques and addresses the problem of accuracy of position estimation. State space model developed for localization is nonlinear and hence does not have a closed form solution. Posterior density for state vector has been derived and simulated using a variant of Kalman Filter and Monte Carlo methods to obtain respective sub-optimal solutions. Least Squared Error approach tries to obtain an estimate that minimizes the squared error whereas and does not reveal any statistical information about the target location. Extended Kalman filter approach tries to estimate the posterior density of target employing approximations of Gaussian state probability distribution and linear state space model and observed to provide better results compared to that of Least Squared Error approach. As the localization model is nonlinear, Extended Kalman filter

approximates it with a linear one by employing Taylor series approximation and if the nonlinearity is severe the accuracy of the algorithm suffers. Particle filter approach also tries to estimate the state posterior density with no restrictions and hence is applicable for any generalized system. In this approach probability density function is approximated using a weighted set of particles drawn using Monte Carlo methods and will enable in computing the all the moments of distribution. Recursive Least Squared Error, Extended Kalman and Sampling Importance Resampling Particle Filtering algorithms are designed for localization and their performances are compared. The performance of Particle filter using Sampling Importance Resampling algorithm is found to be superior to that of Recursive Least Squared Error approach and Extended Kalman filter.

1. INTRODUCTION

RF localization deals with position computation of a wireless device. Research in this field has gained prominence because of its potential applications like E911, navigation, wireless sensor networks, asset tracking, patient monitoring, and many more. GPS navigational tool is one of the most widely used applications employing localization. Position computation is performed based on the behavior of electromagnetic signals used for communication by wireless devices. Many localization techniques have been developed in literature based on electromagnetic signal properties which enable in inferring the location information. Quantities that are of interest in predicting the location of a wireless device are, received signal strength indicator (RSSI) , time of arrival (TOA), and angle of arrival (AOA), associated with it. Existing techniques make use of one or more of the above quantities in estimating target location.

Localization techniques can be classified in different ways depending on the type of information and communication involved. Localization based on type of information used, is classified into range-based and range free techniques. Range-based techniques make use of the range information in determining the target location whereas range free techniques use proximity to known locations. Range-based techniques are based on RSSI, TOA, TDOA (Time Difference of Arrival), AOA and also hybrid techniques which

implement combinations of the above four. Range free techniques are designed primarily for wireless sensor networks which make use of the proximity of a node to anchors for localization.

Localization based on communication involved between wireless devices (nodes) can be classified into active and passive techniques. In active techniques, a node has to communicate with the neighbors or target for position computation. RADAR introduced in [16], employs an active method, where a node transmits an electromagnetic signal and detects the echo signal reflected by target to determine the range. In passive techniques, a node can determine the position of target, without any communication, but by passively listening to the RF emissions present in the environment. MUSIC algorithm in [13], computes the direction or angle of received signal arrival, without any need for communication between transmitter and receiver, which subsequently is used for determining the position.

As range-based techniques rely on distance information from measurements for localization, their estimation accuracy is sensitive to variations in the signal properties which are random because of the fading nature of wireless channels. Fading affects different properties of received signal differently. For instance, RSSI based techniques are most sensitive to shadow fading whereas TOA and AOA based techniques are sensitive to multipath fading. Therefore, one has to maintain caution while choosing the wireless channel models, for obtaining better range estimates.

One common requirement of range based techniques is the measurement of received signal strength. RSSI based techniques measure accurate signal power to infer the range using appropriate path loss models. TOA based techniques also require measurement of signal strength, but its main purpose is to identify the instant of signal arrival and same is the case with TDOA based techniques. In order to determine the range, time of flight (TOF) or propagation time has to be computed, which is possible only when the receiver has knowledge about signal transmission time instant. Also, the receiver and transmitter have to be synchronized for computation of TOF. AOA based techniques also require measurement of received signal strength for identifying the direction of signal arrival. Beam-forming is used to steer the antenna beam and measure RSSI from all possible directions and then identify the direction having maximum value to be the direction of arrival. From the above discussion, one can infer that RSSI technique requires minimum requirements among all range based techniques. Also, RSSI allows localizing a target passively which is not possible with TOA based techniques because of synchronization and TOF computation requirements. AOA based techniques can be used for passive localization but at the cost of increased circuitry, as beam-forming requires an array of antennas. Apart from the above mentioned reasons, RSSI information is readily available from off-the-shelf receivers (e.g. Wi-Fi receivers), making it feasible to apply this technique. This motivates us to adopt localization based on RSSI.

Localization techniques based on RSSI use signal strength indicator received at the measuring station for two purposes (a) to estimate the target range for applying

Trilateration and (b) to generate signatures/fingerprints. In the former case, RSSI is used to infer distance travelled by a signal to reach the receiver, according to a path loss model. Range thus obtained is used in Trilateration for estimating the position. The main drawback of this technique is that its accuracy is sensitive to multipath and shadow fading. Ecolocation in [12], makes use of distance constraints based on RSSI and develop sequences to determine the relative position of transmitter with respect to known reference stations. Disadvantage associated with signature/fingerprint based techniques is that they require large amount of training data and complex algorithms. RSSI based localization using Trilateration is preferred over the signature based technique as it does not require creation of database, and will be the focus of chapter 2.

Besides the above mentioned techniques, localization can be modeled as an estimation problem. Aim of the thesis is to apply Bayesian estimation to passively localize target based on RSSI measurements. Bayesian approach enables in estimating the state posterior density (probability density of system state i.e. target position, conditioned on measurements) using prior information and available measurements. Solution thus obtained is considered to be complete as the estimated state posterior density will integrate all the information about system states. The state space model developed for localization is nonlinear, optimal solution does not have closed form and hence approximations are to be made for obtaining sub-optimal solutions. Two approximation strategies have been explored in this work for constructing the state posterior density. First, an Extended Kalman Filtering is used to approximate the state posterior density with Gaussian and then linearize the nonlinear measurement equation to apply Kalman

Filtering solution. Although this technique does not guarantee optimal solution, it can provide better results if nonlinearity is not severe and is widely used in engineering applications. Recently a new technique has been developed which approximates the state posterior density with Gaussian, represented by a set of points (called sigma points), and then apply these points to original nonlinear state model. This technique is found to give better results compared to Extended Kalman Filter, but the restriction of Gaussian assumption still holds. Second strategy approximates the continuous state posterior density with a weighted set of point masses called particles, obtained by recursively drawing samples from a chosen distribution and then applying recursive Bayesian estimation. Monte Carlo methods have been used to draw random samples such that they closely represent the state posterior density. As it is impossible to draw samples from the state posterior density directly, an importance sampling density is chosen which closely approximates the state posterior density but from which it is easy to draw samples. Samples thus drawn are applied to recursive Bayesian estimation and the accuracy of estimates depends on how closely the importance density follows the actual posterior density. This later approximation is considered to be superior compared to the former as it is applicable for any system with no restrictions either on linearity or probability distribution of state. However, in order to approximate a probability density function accurately, large number of particles are necessary. But, as number of particles increase the computational power required will also increase drastically which, ultimately sets the limit on accuracy achieved. One has to make a trade-off between the required accuracy and computational complexity depending on the application. This work deals with

application of Least Squared Error Filter (LSF) using Trilateration, Extended Kalman Filter (EKF) and Particle Filter (PF) for localization and compares their performances.

Organization of the thesis is as follows. Chapter 2 provides background information about behavior of electromagnetic signals in wireless channels and the significance of path loss models in range computation. Basic techniques for localization are described and Trilateration is demonstrated mathematically for free space and mobile wireless channels. Least Squared Error Filtering (LSF) and its recursive version (RLSF) are analyzed and simulation results are presented. Because of the limited knowledge of the LSF, a more generalized method for state estimation is desired and hence Bayesian approach for state estimation has been used. Chapter 3 deals with introduction to nonlinear Bayesian estimation. As the state space model developed for localization based on RSSI is nonlinear, approximate solutions are explored in chapters 4 and 5. Application of Extended Kalman Filter (EKF) is explored and its simulation results are presented in chapter 4. Chapter 5 introduces Monte Carlo estimation and importance sampling. Sequential Importance Sampling (SIS) and its variant Sampling Importance Resampling (SIR) algorithms, used for constructing the state posterior density, will be presented along with simulation results for SIR algorithm. Thesis concludes with chapter 6 presenting the comparison results of RLSF, EKF and Particle Filter using SIR algorithms for localization.

2. BACKGROUND

This chapter provides the required background for localization based on RSSI employing Trilateration. As mentioned in chapter 1, Trilateration makes use of distance information for estimating the target location. Distance information in general, is not directly available and hence needs to be inferred from the measurements available. For localization based on RSSI, power of the received signal has to be measured; using which, distance travelled by the signal can be inferred based on appropriate path loss models. Accuracy of position estimates is dependent on the distance inferred using a path loss model and hence it is worth discussing the theory behind development of path loss models.

Electromagnetic Propagation

From antenna theory, it is known that the radiation component of electric field is inversely proportional to the distance between source and measured point.

$$E \propto \frac{1}{d} \qquad (2.1)$$

Also, power is proportional to square of the electric field.

$$P \propto E^2 \qquad (2.2)$$

Therefore power is inversely proportional to the square of the distance.

$$P \propto \frac{1}{d^2} \qquad (2.3)$$

Ideally, an isotropic antenna radiates power equally in all directions. Locus of points having equal power at distance d units from the source is a sphere of radius d. For free space propagation, losses are assumed to be non existent because of the absence of obstacles. Therefore, signal power along a sphere of radius d will equal that at source. Although total signal power remains same, its density at a point on the surface of sphere gets reduced proportional to d^2. Contrary to the free space case, mobile wireless medium consists of obstacles and hence losses are prevalent which affect the signal power received at a point d units from source. Many models characterizing the path loss have been developed in literature.

2.1 Free-Space Propagation Model

The channel model is based on variations of transmitted signal power when propagated through a free space medium. Assume that an isotropic antenna transmits electromagnetic signal of power P_t in to the free space with signal power being distributed equally in all directions. Power density of the signal at a point d units distant from the transmitter is given by

$$P_d = \frac{P_t}{4\pi d^2} \qquad (2.4)$$

As it is impossible to implement isotropic antenna in practice, we compensate by assuming a directive antenna with gain G_t. So, the power density P_d is given by

$$P_d = \frac{P_t G_t}{4\pi d^2} \qquad (2.5)$$

Now if a receiver antenna is placed at that point, then the power incident on receiving antenna denoted by P_r is given by

$$P_r = P_d A_e \qquad (2.6)$$

Where A_e is the antenna aperture and is expressed as

$$A_e = \frac{G_r}{4\pi\lambda^2} \qquad (2.7)$$

Where λ is the wavelength of the transmitted signal

G_r is gain of the receiving antenna

Expression to determine the received power at a distance d units from the transmitter in free space is given by

$$P_r = P_t G_t G_r \left(\frac{\lambda}{4\pi d}\right)^2 \qquad (2.8)$$

The term $P_t G_t$ is called Effective Isotropic Radiated Power (EIRP) and the term $\left(\frac{\lambda}{4\pi d}\right)^{-2}$ is called free space path loss.

2.2 Uncertainties in Mobile Wireless Medium

Free space propagation model discussed in the previous section is not applicable to mobile radio environment, as it assumes a medium free of obstacles and hence its path loss is dependent only on distance d and wavelength λ. In real world cases, apart from distance path loss also depends on local terrain characteristics, antenna heights. Therefore a need for developing path loss model arises, which accounts for all the losses. Whenever an electromagnetic wave propagates through wireless medium, it experiences

(i) Decrease in power level due to path loss

(ii) Random variations due to multipath and mobility

Because of the above effects, received signal at a measuring station will have reduced power with random variations and hence the models used to characterize wireless channels are often statistical in nature. This phenomenon of randomness introduced by channel is called fading categorized into two types namely 'Fast/Small-scale fading' and 'Slow/Large-scale fading'.

Fast/Small-scale fading is caused due to multi-path propagation of electromagnetic signals. Multi-path propagation arises because of the phenomena of reflection, diffraction, scattering during the propagation of electromagnetic signals in the presence of obstacles, which results in generation of multiple replicas of transmitted signal. Replicas of transmitted signal propagate through different paths and arrive at receiver at different time instants with different amplitudes which when combined result in a highly

distorted version of the original signal with random fluctuations. Because of this fading, instantaneous received signal level varies drastically within a distance of the order of transmitted signal wavelength and also it is difficult to retrieve information from it. If the received power is averaged over an interval of time/distance, fast fading can be eliminated.

Slow/Large-scale fading is mainly caused due to the terrain configuration of area surrounding transmitter and receiver. Transmitted electromagnetic signal interacts with each obstacle along its transit and looses a fraction of its energy. Number of obstacles that that interact with a signal propagating through the wireless medium is random and hence the power received becomes a random quantity. Two paths having same distance with different terrain configurations will have different received power values measured at the receiver. Large scale fading is independent of time and hence cannot be eliminated by averaging as in the case of small scale fading. Loss of transmitted signal power because of obstacles and propagation distance can be characterized using path loss models.

Fading affects the basic model of Trilateration in two ways.

1. Measured receiver positions will be random
2. Measured power will be random

From GPS measurements it has been observed that the position coordinates follow Gaussian distribution. In order to obtain an estimate of the actual measurement points parameters of the observed probability distribution has to be computed. Fortunately as the position coordinates follow Gaussian distribution, optimal estimator (Minimum variance unbiased estimator) is the sample mean.

2.2.1. Random variable to characterize the received power

Effect of obstacles on the signal power is multiplicative and is best characterized by a Log-normal distribution in linear scale or Gaussian distribution in logarithmic scale. From the measurements performed, it has been observed that received power indeed follows Gaussian distribution in logarithmic scale. Although, the effect of small scale fading can be negated by averaging, large scale fading primarily determines the signal power deterioration as the signal propagates through the wireless medium. In order to characterize the large scale fading, path loss models have been developed for various environments.

Generalized Empirical path-loss model

$$L_p(d) = L_p(d_0) + 10\eta \log_{10}(d) + \varepsilon \qquad (2.9)$$

Where $L_p(d)$ is the path loss at distance d

d_0 denotes a reference distance e.g., 1m, 10m, and 100m

η is the path-loss exponent

d is the distance between transmitter and the receiver

ε is a zero mean Gaussian random variable

This model can be applied successfully to various environments by appropriately choosing the values of η and standard deviation ε. Typical values of η and ε are in the range of 2 – 6, and 3 – 12 dB respectively. Once the path loss is obtained, received power equation can be computed as shown below.

$$P_r = P_t + G_t + G_t - L_p(d) \qquad (2.10)$$

Where P_r and P_t are the received and transmitted powers

G_t and G_r are the transmit and receive antenna gains respectively

Thus the received power will be a random quantity and is characterized by the randomness of $L_p(d)$. The quantities denoted in equation (2.10) are on dB scale.

2.3 Basic Techniques for Localization

Using the range information obtained by various means mentioned above, one of the following described techniques is applied to compute the position.

2.3.1 Trilateration

In this technique, relative position of the target is determined using the range information of target from reference points. Suppose P is the point at which target is located, and consider three reference points A, B & C that are at distances of d_1, d_2 & d_3 respectively from the target. At location A, the probable region within which the target (at a distance of d_1) can reside is a circle of radius d_1. Similarly, region where the target can reside observing from locations B & C are also circles with radius d_2 & d_3 respectively. Then, target location can be determined as the point of intersection of three circles with centers at A, B and C as depicted in figure 1. Method described here is for locating a target in a two dimensional plane. If the target has location has to be estimated in a three dimensional space, then the location of target is the intersection of spheres from each of the measured locations.

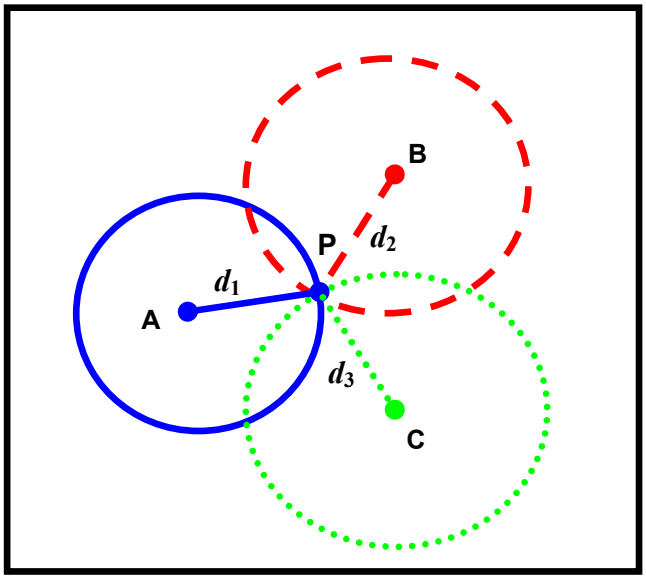

Figure 1 : Illustration of Trilateration

2.3.2 Triangulation

In this technique, position of target is determined using a combination of range and angle information. Let points A, B and C be the vertices of a triangle with target located at one of the vertices, say C. Assuming that locations of A and B are known and denoting the angles subtended to the target C from other vertices be α and β respectively. Using the axiom that sum of angles in a triangle is 180^0 (degrees), the angle at C is obtained by $180 - \alpha - \beta$. Law of sines (alternatively law of cosines) is applied to determine the other sides of triangle as shown below.

$$\frac{\text{Sin}(180\text{-}\alpha\text{-}\beta)}{\text{AB}} = \frac{\text{Sin}(\alpha)}{\text{BC}} = \frac{\text{Sin}(\beta)}{\text{CA}} \qquad (2.11)$$

Once length of the sides BC and CA is known, coordinates of target can be computed as the intersection of arcs from A and B with lengths BC and CA. This technique is illustrated using figure 2.

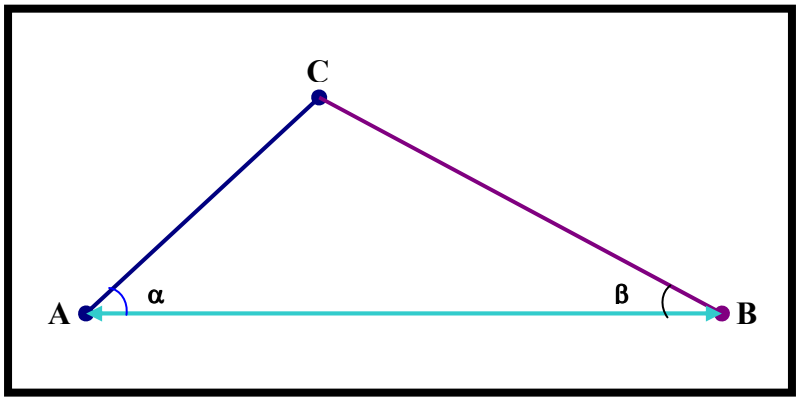

Figure 2 : Illustration of Triangulation

2.3.3 Multilateration

Position of target is determined using time difference of arrivals (TDOA) of the transmitted signal, at three different receivers. This is also called as hyperbolic positioning which will be evident shortly. Let A, B, and C be the reference points and X the location of target in a three dimensional plane. If distances to reference points from X are obtained using time of arrival information, then following equations are obtained.

$$
\begin{aligned}
T_A &= \frac{1}{c}\sqrt{(x-x_A)^2+(y-y_A)^2+(z-z_A)^2} \\
T_B &= \frac{1}{c}\sqrt{(x-x_B)^2+(y-y_B)^2+(z-z_B)^2} \\
T_C &= \frac{1}{c}\sqrt{(x-x_C)^2+(y-y_C)^2+(z-z_C)^2}
\end{aligned}
\tag{2.12}
$$

The time differences are computed from the time of arrivals which result in equations of hyperbolas as given in equation (2.13).

$$
\begin{aligned}
\tau_{AB} &= T_A - T_B = \frac{1}{c}\{\sqrt{(x-x_A)^2+(y-y_A)^2+(z-z_A)^2} - \sqrt{(x-x_B)^2+(y-y_B)^2+(z-z_B)^2}\} \\
\tau_{BC} &= T_B - T_C = \frac{1}{c}\{\sqrt{(x-x_B)^2+(y-y_B)^2+(z-z_B)^2} - \sqrt{(x-x_C)^2+(y-y_C)^2+(z-z_C)^2}\} \\
\tau_{CA} &= T_C - T_A = \frac{1}{c}\{\sqrt{(x-x_C)^2+(y-y_C)^2+(z-z_C)^2} - \sqrt{(x-x_A)^2+(y-y_A)^2+(z-z_A)^2}\}
\end{aligned}
\tag{2.13}
$$

The point of intersection of two hyperbolas gives the position co-ordinates of the target in a two-dimensional space as depicted in figure 3. For estimation in a three dimensional space, four or more reference point measurements have to be included to achieve better accuracy.

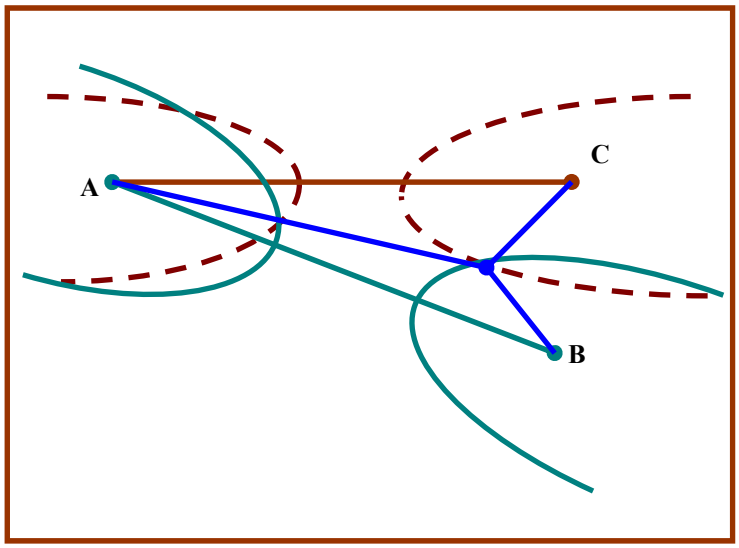

Figure 3 : Illustration of Multilateration

In general, intersection of the circles/arcs/hyperbolas does not coincide exactly because of uncertainties in the model used for range/time/angle estimation; as a result solution is an overlapped area but not a point, where the target can reside. Accuracy of a technique is determined by the intersection region and is proportional to its area. By increasing the number of measurements, accuracy of location estimation can be improved by reducing the overlapping area. Position estimate in this area can be obtained using any of the schemes like least squared error solution or if the position follows a probability distribution, then the maximum likelihood estimate can be computed.

2.4 Trilateration

As Triangulation and Multilateration described in the above sections require either AOA or TOA information, it is difficult to apply them for localization using RSSI and hence are not considered. From the discussion of electromagnetic propagation and path loss models thereafter introduced, relationship between distance and power received has been established. This relation is used to deduce the distance information from signal power measured at random selected points within the coverage area of target. At each of the measurement locations, appropriate path loss model will be applied to compute the distance used in Trilateration to determine target location. Here, the underlying assumption is that position of the measurement points is known; which can be obtained independently by measurements.

The locus of points which are equidistant from a fixed point is a circle in two dimensional plane and is a sphere in 3 dimensional space. Once the distance estimate is obtained, then the location of target can be anywhere along the circle/sphere with radius equal to the distance d between the target and measured position.

2.4.1 Trilateration for free-space

Let (x_1, y_1) and (x_2, y_2) be the measurement locations and P_1, P_2 be the power received at respective locations. Using the free space power equation (2.8), distance from the targets can be computed, denoted by d_1 and d_2. Then the coordinates (x, y) of target satisfy the following equations.

$$\begin{aligned}(x-x_1)^2+(y-y_1)^2&=d_1{}^2\\(x-x_2)^2+(y-y_2)^2&=d_2{}^2\end{aligned}\qquad(2.14)$$

If the coordinates are so chosen that $y_1 = y_2$, then x is obtained by subtracting one equation from the other, and by back substitution y can be determined.

$$x=\frac{\sqrt{d_1{}^2-d_2{}^2+x_2{}^2-x_1{}^2}}{2(x_2-x_1)}\qquad(2.15)$$

$$y=y_1\pm\sqrt{d_1{}^2-(x-x_1)^2}\qquad(2.16)$$

Value of y which satisfies both the circle equations is the solution. This method can be extended to three dimensional case (3D) as well. If it is possible to obtain more number of readings than the dimensions of position vector, following method can also be employed. Suppose 4 equations are obtained from as many different locations in a 3D space, as given in (2.17).

$$\begin{aligned}(x-x_1)^2+(y-y_1)^2+(z-z_1)^2&=d_1{}^2\\(x-x_2)^2+(y-y_2)^2+(z-z_2)^2&=d_2{}^2\\(x-x_3)^2+(y-y_3)^2+(z-z_3)^2&=d_3{}^2\\(x-x_4)^2+(y-y_4)^2+(z-z_4)^2&=d_4{}^2\end{aligned}\qquad(2.17)$$

The above set of equations can be solved by subtracting one equation from the proceeding one and hence equations which are linear in (x, y, z) will be obtained. The above set of linear equations can be easily solved using linear algebra.

$$\begin{bmatrix} x_2 - x_1 & y_2 - y_1 & z_2 - z_1 \\ x_3 - x_2 & y_3 - y_2 & z_3 - z_2 \\ x_4 - x_3 & y_4 - y_3 & z_4 - z_3 \end{bmatrix} \times \begin{bmatrix} x \\ y \\ z \end{bmatrix} = \begin{bmatrix} d_1^2 - d_2^2 + x_2^2 - x_1^2 \\ d_2^2 - d_3^2 + x_3^2 - x_2^2 \\ d_3^2 - d_1^2 + x_4^2 - x_3^2 \end{bmatrix} \qquad (2.18)$$

As this is an idealistic model, results obtained are quite accurate with zero error.

2.4.2 Trilateration for mobile wireless medium

In this section, application of Trilateration for mobile wireless medium will be described. Using the same set of equations of (2.18), with a change in notation can be represented be represented as a model given in equation (2.19).

$$HX = Y \qquad (2.19)$$

Where,

$$H = \begin{bmatrix} x_2 - x_1 & y_2 - y_1 & z_2 - z_1 \\ x_3 - x_2 & y_3 - y_2 & z_3 - z_2 \\ x_4 - x_3 & y_4 - y_3 & z_4 - z_3 \end{bmatrix} \qquad (2.20)$$

$$X = \begin{bmatrix} x \\ y \\ z \end{bmatrix} \qquad (2.21)$$

$$Y = \begin{bmatrix} d_1^2 - d_2^2 - (x_1^2 + y_1^2 + z_1^2) + (x_2^2 + y_2^2 + z_2^2) \\ d_2^2 - d_3^2 - (x_2^2 + y_2^2 + z_2^2) + (x_3^2 + y_3^2 + z_3^2) \\ d_3^2 - d_4^2 - (x_3^2 + y_3^2 + z_3^2) + (x_4^2 + y_4^2 + z_4^2) \end{bmatrix} \qquad (2.22)$$

Quantities d_i, $i = 1,2,3,4$ in (2.22) are random variables and coordinates (x_i, y_i, z_i) in (2.20 & 2.22) are the estimates of measured location coordinates. The solution for (x, y, z) is obtained from equation (2.23).

$$\hat{X} = H'T \qquad (2.23)$$

Where, H' and T are defined as in (2.24) and (2.25).

$$H' = \begin{bmatrix} R_{11} & R_{12} - R_{11} & R_{13} - R_{12} & R_{13} \\ R_{21} & R_{22} - R_{21} & R_{23} - R_{22} & R_{23} \\ R_{31} & R_{32} - R_{31} & R_{33} - R_{32} & R_{33} \end{bmatrix} \qquad (2.24)$$

$R_{ij} =$ element in i^{th} row and j^{th} column of matrix R. Where $R = A^{-1}$

$$T = \begin{bmatrix} d_1^{\,2} - (x_1^{\,2} + y_1^{\,2} + z_1^{\,2}) \\ d_2^{\,2} - (x_2^{\,2} + y_2^{\,2} + z_2^{\,2}) \\ d_3^{\,2} - (x_3^{\,2} + y_3^{\,2} + z_3^{\,2}) \\ d_4^{\,2} - (x_4^{\,2} + y_4^{\,2} + z_4^{\,2}) \end{bmatrix} \qquad (2.25)$$

Solutions for the individual coordinates are of the form in equation (2.26). Each variable can be represented as weighted sum of the squares of distances and norms obtained from each measured point.

$$
\begin{aligned}
x &= R_{11}(d_1{}^2 - Norm_1{}^2) + (R_{12} - R_{11})(d_2{}^2 - Norm_2{}^2) + (R_{13} - R_{12})(d_3{}^2 - Norm_3{}^2) \\
&+ R_{13}(d_4{}^2 - Norm_4{}^2) \\
y &= R_{21}(d_1{}^2 - Norm_1{}^2) + (R_{22} - R_{21})(d_2{}^2 - Norm_2{}^2) + (R_{23} - R_{22})(d_3{}^2 - Norm_3{}^2) \\
&+ R_{23}(d_4{}^2 - Norm_4{}^2) \\
z &= R_{31}(d_1{}^2 - Norm_1{}^2) + (R_{32} - R_{31})(d_2{}^2 - Norm_2{}^2) + (R_{33} - R_{32})(d_3{}^2 - Norm_3{}^2) \\
&+ R_{33}(d_4{}^2 - Norm_4{}^2)
\end{aligned}
\tag{2.26}
$$

Where $Norm_i{}^2 = x_i{}^2 + y_i{}^2 + z_i{}^2$

As the solution of position vector is available, probability distribution of random vector (x, y, z) can be obtained. Since the vectors (x_i, y_i, z_i) are observed to be Gaussian (Material on distributions can be found in [2]), their norms follows either Rayleigh or Rician distribution, depending on the variances of individual position coordinates. Rician random variable is a better choice for characterizing norm as it also includes Rayleigh distribution as its special case. Square of the norm follows chi-square distribution with 3 degrees of freedom.

Probability distribution of distance d_i can be derived using the path-loss model provided received power is known. Conditional probability distribution of distance given received power has been observed to follow log-normal distribution. The probability distribution of coordinates (x, y, z) becomes complex as it involves convolution of multiple log-normal and chi-square random variables which is not analytically tractable and hence the distribution obtained will not have closed form solution.

2.5 Least Squared Error Solution

Equations in the Trilateration are inconsistent because of the random errors in measurement of power which in turn reflect in the distances computed. If there is no knowledge about the behavior of errors, least squared solution is the most desired for system of equations. Therefore, one needs to have large number of measurements to compute the least square solution. Two desirable properties of the resulting least squares error solution are that its mean is unbiased and have minimum variance.

Suppose N measurements are obtained at as many different locations, then N equations are obtained. Modifying the equations as in (2.18), a set of linear simultaneous equations represented in the matrix form as in (2.19) are obtained. As the system now is over-determined and elements in the matrices are modified to equations (2.27) and (2.28).

$$H = \begin{bmatrix} x_2 - x_1 & y_2 - y_1 & z_2 - z_1 \\ x_3 - x_2 & y_3 - y_2 & z_3 - z_2 \\ x_4 - x_3 & y_4 - y_3 & z_4 - z_3 \\ . & . & . \\ . & . & . \\ . & . & . \\ x_N - x_{N-1} & y_N - y_{N-1} & z_N - z_{N-1} \end{bmatrix} \qquad (2.27)$$

$$X = \begin{bmatrix} x \\ y \\ z \end{bmatrix}$$

$$Y = \begin{bmatrix} d_1^2 - d_2^2 - (x_1^2 + y_1^2 + z_1^2) + (x_2^2 + y_2^2 + z_2^2) \\ d_2^2 - d_3^2 - (x_2^2 + y_2^2 + z_2^2) + (x_3^2 + y_3^2 + z_3^2) \\ d_3^2 - d_4^2 - (x_3^2 + y_3^2 + z_3^2) + (x_4^2 + y_4^2 + z_4^2) \\ . \\ . \\ . \\ d_{N-1}^2 - d_N^2 - (x_{N-1}^2 + y_{N-1}^2 + z_{N-1}^2) + (x_N^2 + y_N^2 + z_N^2) \end{bmatrix} \quad (2.28)$$

Least squared solution for the above determined set of equations is of the form as given in equation (2.29).

$$\hat{X} = (H^T H)^{-1}(H^T Y) \quad (2.29)$$

Let $R = (H^T H)^{-1} H^T$ which is a $3 \times N$ matrix. Perform elementary operations on R such that the resultant solution of X is of the form as shown below.

$$X = R' \times D - R' \times Norm \quad (2.30)$$

Where R' is the matrix obtained after applying elementary operations.

$$D = \begin{bmatrix} d_1^2 & d_2^2 & d_3^2 & d_4^2 & . & . & d_N^2 \end{bmatrix}^T$$

$$Norm = \begin{bmatrix} Norm_1^2 & Norm_2^2 & Norm_3^2 & Norm_4^2 & . & . & Norm_N^2 \end{bmatrix}^T$$

Solution for the individual coordinates is of the form given by equation (2.31).

$$
\begin{aligned}
x &= R_{11} \times (d_1^2 - Norm_1^2) + \sum_{i=2}^{N} (R_{1i} - R_{1(i-1)}) \times (d_i^2 - Norm_i^2) + R_{1N} \times (d_N^2 - Norm_N^2) \\
y &= R_{21} \times (d_1^2 - Norm_1^2) + \sum_{i=2}^{N} (R_{2i} - R_{2(i-1)}) \times (d_i^2 - Norm_i^2) + R_{2N} \times (d_N^2 - Norm_N^2) \\
z &= R_{31} \times (d_1^2 - Norm_1^2) + \sum_{i=2}^{N} (R_{3i} - R_{3(i-1)}) \times (d_i^2 - Norm_i^2) + R_{3N} \times (d_N^2 - Norm_N^2)
\end{aligned}
\qquad (2.31)
$$

Assuming perfect knowledge of measurement points, variables (x, y, z) are simply weighted sum of the random variables d_i^2. As the number of measurement points increase, distributions of the target location variables tend towards Gaussian according to the central limit theorem.

2.5.1 Error in Position Estimation

In this section, error distribution in estimating variable location by least squared solution is analyzed. As the power measured is a random associated with errors, distance estimated using this measurement also suffers from error. Suppose d_{i0} and d_i be the actual and estimated distances between the measurement location and the target. Ideally, if there were no shadowing, received signal power is given by

$$P_r = P_t + G_t + G_r - L_p(d_0) \qquad (2.32)$$

Where $L_p(d_0) = L_p(d_{00}) + 10\eta \log_{10}(d_0)$

If the shadowing effect has to be accounted for in received power equation, then the above path loss equation will be modified to

$$L_p(d) = L_p(d_{00}) + 10\eta \log_{10}(d_0) + \varepsilon \quad (2.33)$$

Where $\varepsilon = \mathrm{N}(0, \sigma)$

Rearranging the received power equation (2.32) for distance as

$$d = 10^{\frac{1}{10\times\eta}[Pt+Gt+Gr-Lp(d_{00})-\varepsilon]} \quad (2.34)$$

Representing the estimated distance in terms of original distance d_0 as

$$d = d_0 10^{\frac{\varepsilon}{10\times\eta}} \quad (2.35)$$

$$d = d_0 e^{\frac{2.303\times\varepsilon}{10\times\eta}} \quad (2.36)$$

Let $k = \frac{2.303\varepsilon}{10\eta}$ be the exponent of noise term. Expanding the exponential term

$$d = d_0(1 + k + \frac{k^2}{2} + ...) \quad (2.37)$$

In general, the value of k is small, hence it is a good approximation to neglect higher order terms in the series (terms with exponent $k \geq 2$). Therefore, the approximated distance is given as

$$d = d_0 + d_0 \times k \quad (2.38)$$

Let X_0 and X be the original and estimated position vectors. Then error in estimating the position is obtained using (2.30).

$$e = X_0 - X \quad (2.39)$$

$$e = (R' \times D_0 - R' \times Norm) - (R' \times D - R' \times Norm) \qquad (2.40)$$

Where

$$D_0 = \begin{bmatrix} d_{10}^{\,2} & d_{20}^{\,2} & d_{30}^{\,2} & d_{40}^{\,2} & . & . & d_{N0}^{\,2} \end{bmatrix}^T$$

$$e = R' \times (D_0 - D) \qquad (2.41)$$

$$\begin{aligned} e_x &= R_{11} \times (d_{10}^{\,2} - d_1^{\,2}) + \sum_{i=2}^{N} (R_{1i} - R_{1(i-1)}) \times (d_{i0}^{\,2} - d_i^{\,2}) + R_{1N} \times (d_{N0}^{\,2} - d_N^{\,2}) \\ e_y &= R_{21} \times (d_{10}^{\,2} - d_1^{\,2}) + \sum_{i=2}^{N} (R_{2i} - R_{2(i-1)}) \times (d_{i0}^{\,2} - d_i^{\,2}) + R_{2N} \times (d_{N0}^{\,2} - d_N^{\,2}) \\ e_z &= R_{31} \times (d_{10}^{\,2} - d_1^{\,2}) + \sum_{i=2}^{N} (R_{3i} - R_{3(i-1)}) \times (d_{i0}^{\,2} - d_i^{\,2}) + R_{3N} \times (d_{N0}^{\,2} - d_N^{\,2}) \end{aligned} \qquad (2.42)$$

Now substituting the approximated distances in equation (2.42), error in individual coordinates can be given as

$$\begin{aligned} e_x &= R_{11} \times (d_{10}^{\,2} \times (2 \times k + k^2)) + \sum_{i=2}^{N} (R_{1i} - R_{1(i-1)}) \times (d_{i0}^{\,2} \times (2 \times k + k^2)) + R_{1N} \times (d_{N0}^{\,2} \times (2 \times k + k^2)) \\ e_y &= R_{21} \times (d_{10}^{\,2} \times (2 \times k + k^2)) + \sum_{i=2}^{N} (R_{2i} - R_{2(i-1)}) \times (d_{i0}^{\,2} \times (2 \times k + k^2)) + R_{2N} \times (d_{N0}^{\,2} \times (2 \times k + k^2)) \\ e_z &= R_{31} \times (d_{10}^{\,2} \times (2 \times k + k^2)) + \sum_{i=2}^{N} (R_{3i} - R_{3(i-1)}) \times (d_{i0}^{\,2} \times (2 \times k + k^2)) + R_{3N} \times (d_{N0}^{\,2} \times (2 \times k + k^2)) \end{aligned} \qquad (2.43)$$

2.6 Simulation Results

The simulation parameters used for LSF are given below

Shadowing standard deviation $\sigma_1 = 6dB$

Path loss exponent $\eta = 4$

It has been observed from simulations that, as the number of measurement points increase error tends towards zero. It assumes perfect knowledge of transmission parameters and measurement locations. Simulation results are shown in the following figures 4 and 5 for varying number of measurement locations. Figure 4 captures the error performance in determining the location whereas figure 5 indicates the error in individual coordinates. Figure 6 provides the average error performance with number of measurement locations.

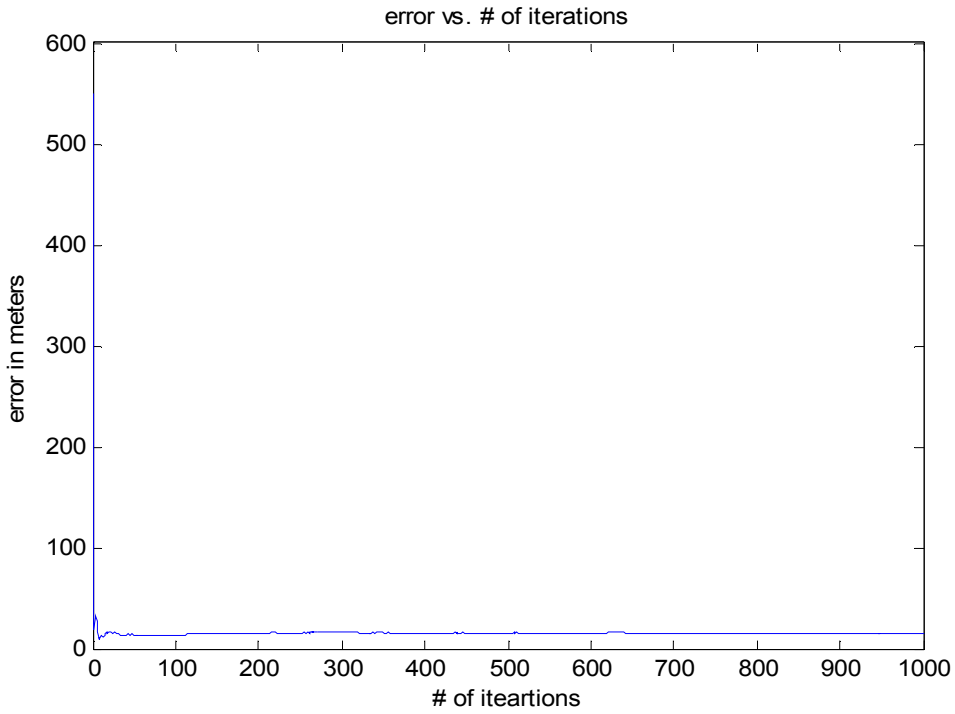

Figure 4 : Plot of LSF Error vs. Number of Iterations

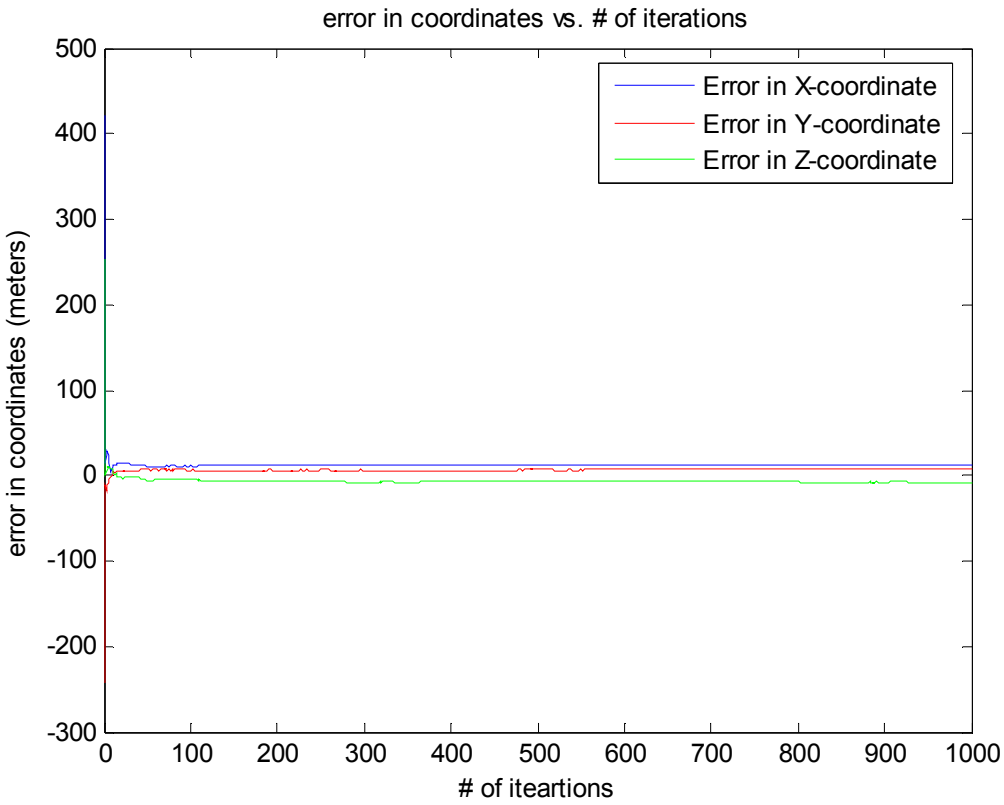

Figure 5 : Plot of LSF Error in Coordinates vs. Number of Iterations

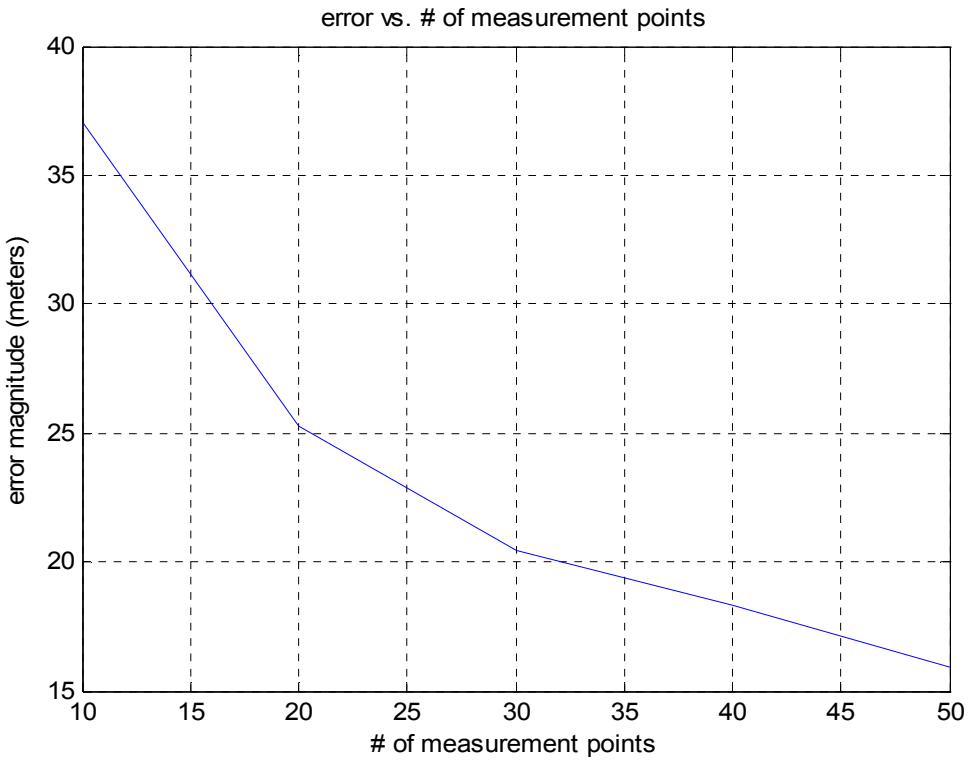

Figure 6 : Plot of Average LSF Error (meters) vs. Number Locations

For each of measurement location number, simulation has been run for 100 times and the results are averaged. Main difficulty with the above form of direct solution involves computation of inverses for matrices of order $N \times N$, N being the number of measurements. As the number of measurement locations increases, number of operations required will increase at the rate of $O\left(N^3\right)$. In order to overcome this computational difficulty, one would like to have least squared solution in a recursive form, which reduces the number of operations performed to $O\left(N \times n^2\right)$ as mentioned in [3]. Where, n is the dimension of position vector.

2.7 Recursive Least Squared Filtering

To formulate this problem, let us consider that one has the knowledge of system at time $i-1$ represented by the equation (2.44).

$$Y_{i-1} = H_{i-1}\hat{X}_{i-1} \qquad (2.44)$$

At time i, let $y(i)$ and $h(i)$ be the new set of observation and transformation values respectively. Set of equations including the new measurements can be represented by

$$Y_i = H_i\hat{X}_i \qquad (2.45)$$

or

$$\begin{bmatrix} Y_{i-1} \\ y(i) \end{bmatrix} = \begin{bmatrix} H_{i-1} \\ h(i) \end{bmatrix}\hat{X}_i \qquad (2.46)$$

Then the solution for $\hat{X}_i$ is of the form

$$\hat{X}_i = \left(\begin{bmatrix} H_{i-1} \\ h(i) \end{bmatrix}^T \begin{bmatrix} H_{i-1} \\ h(i) \end{bmatrix} \right)^{-1} \begin{bmatrix} H_{i-1} \\ h(i) \end{bmatrix}^T \begin{bmatrix} Y_{i-1} \\ y(i) \end{bmatrix} \qquad (2.47)$$

Where $[\ ]^T$ represents the transpose operation. Modifying the above equation, $\hat{X}_i$ is obtained as

$$\hat{X}_i = \left({H_{i-1}}^T H_{i-1} + h(i)^T h(i) \right)^{-1} \left({H_{i-1}}^T Y_{i-1} + h(i)^T y(i) \right) \qquad (2.48)$$

If initial conditions Π_0^{-1} are to be considered, then the above equation has to be modified as given by equation (2.49).

$$\hat{X}_i = \left(\Pi_0^{-1} + H_{i-1}^T H_{i-1} + h(i)^T h(i)\right)^{-1}\left(H_{i-1}^T Y_{i-1} + h(i)^T y(i)\right) \qquad (2.49)$$

$$\hat{X}_i = P_i\left(H_{i-1}^T Y_{i-1} + h(i)^T y(i)\right) \qquad (2.50)$$

Where, $P_i = \left(\Pi_0^{-1} + H_i^T H_i\right)^{-1}$ (2.51)

One can infer the recursive relation

$$H_i^T H_i = \left(H_{i-1}^T H_{i-1} + h(i)^T h(i)\right) \qquad (2.52)$$

Above equation can also be written as

$$P_i^{-1} = P_{i-1}^{-1} + h(i)^T h(i) \qquad (2.53)$$

Using Woodbury matrix identity given in equation (2.54) for the above recursive equation (2.53) and rearranging results in equation (2.55)

$$(A + BCD)^{-1} = A^{-1} - A^{-1}B\left(C^{-1} + DA^{-1}B\right)^{-1}DA^{-1} \qquad (2.54)$$

$$P_i = P_{i-1} - \frac{P_{i-1}h(i)^T h(i)P_{i-1}}{1 + h(i)P_{i-1}h(i)^T} \qquad (2.55)$$

$$P_i = P_{i-1}\left(I - Kh(i)\right) \qquad (2.56)$$

Where, $K = \dfrac{P_{i-1}h(i)^T}{1 + h(i)P_{i-1}h(i)^T}$ (2.57)

Substituting P_i in equation for $\hat{X}_i$ in equation (2.50) and after manipulations, recursive solution for least squared estimate is obtained as given by (2.58).

$$\hat{X}_i = \hat{X}_{i-1} + \frac{P_{i-1}h(i)^T}{1 + h(i)P_{i-1}h(i)^T}\left(y(i) - h(i)^T\,\hat{X}_{i-1}\right) \qquad (2.58)$$

Equation (2.58) constitutes the recursive solution using deterministic least squared error criterion. Direct (batch) and recursive (sequential) solutions are simulated and the results are plotted in figures 7 and 8. Figure 7 simulates LSF and RLSF assuming absence of shadowing where as simulation in figure 8 uses the parameters of least squared error solution. From the simulations it can be verified that both batch and sequential solutions provide identical error performance. The reason for adopting recursive solution is to reduce the computational and memory costs without affecting the error performance.

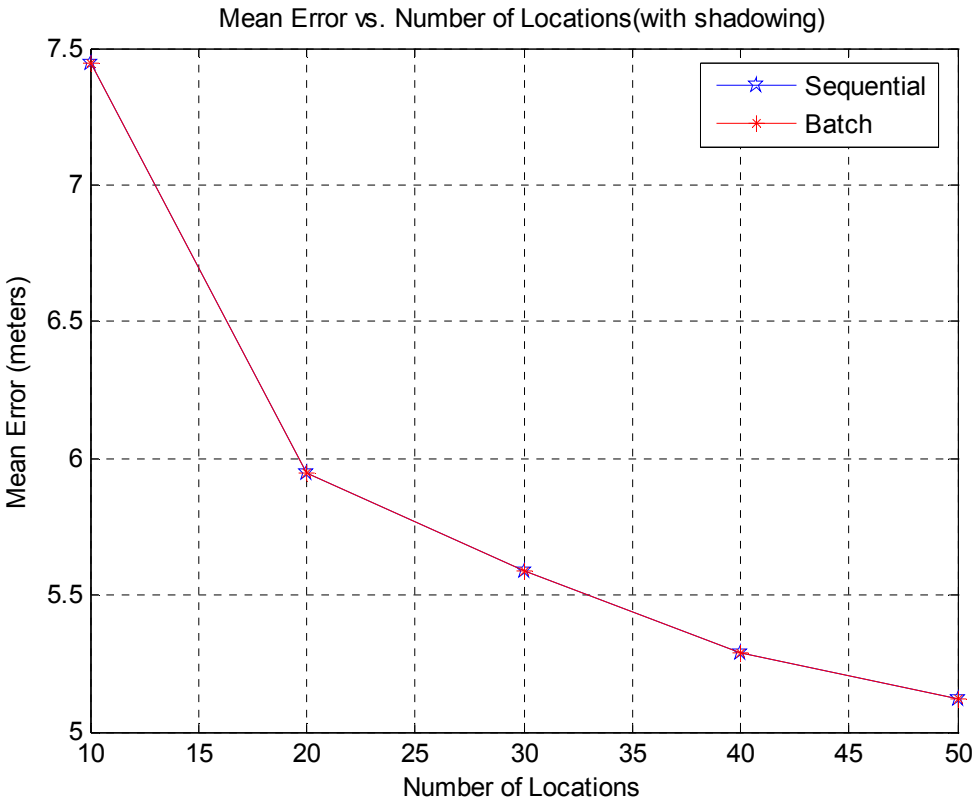

Figure 7: Plot of Average LSF and RLSF Error vs. Number of Measurement Locations

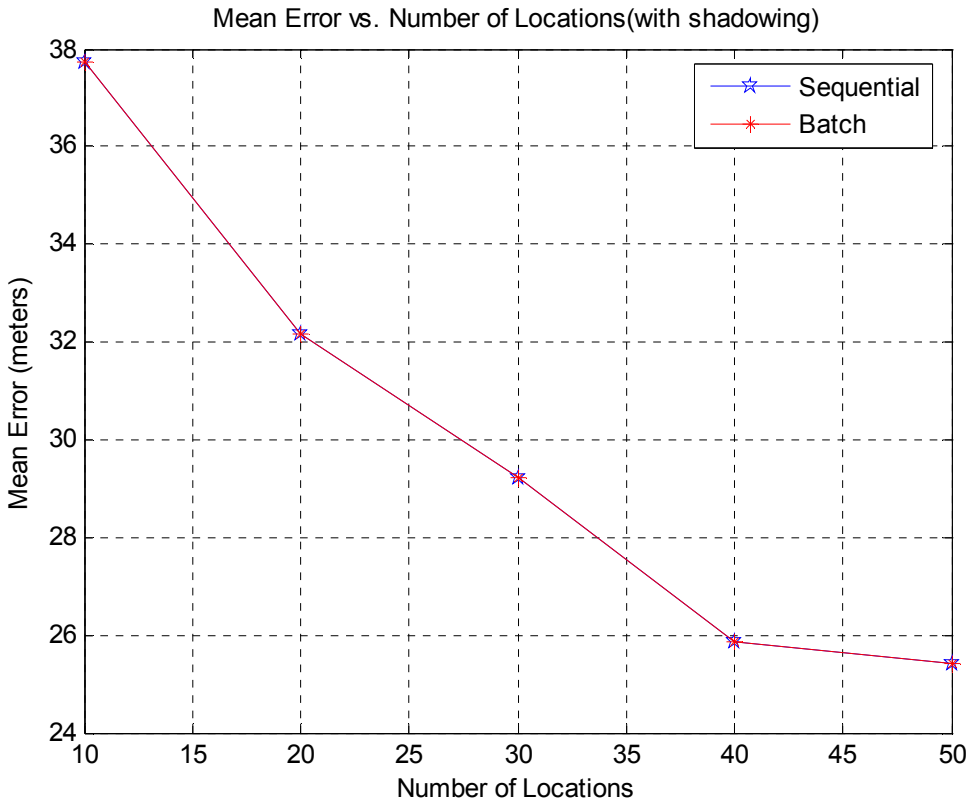

Figure 8 : Plot of Average Error vs. Number of Measurement Locations (Shadowing)

3. LOCALIZATION USING BAYESIAN ESTIMATION

The least squared error solution approach generates an estimate that minimizes the squared error but does not provide any statistical information regarding the target location. It is obvious that an estimate with a single value does not provide as much information as an estimate which is represented probabilistically over a range of values. Thus a solution which can provide the probability density of target in a region is desired and hence estimation using Bayesian approach has been explored. Bayesian estimation/tracking attempts to construct posterior probability density of system based on prior information and available measurements. Posterior density thus obtained is considered to be a complete solution as it embeds all the statistical information about system states. Possibility of such a construction requires definition of a state space model, consisting of state dynamic equation characterizing the evolution of system states with time and a measurement equation describing the relation between measured quantities and the state of system.

3.1 State Space Model

Any dynamic system can be represented in terms of state space model derived from physics of that system. State space model is described by a pair of equations as in (3.1),

consisting of state dynamic and measurement equations. Suppose a system is defined by an n^{th} order differential equation, then its state space is completely described by a vector consisting of n state variables. Let p be the number of outputs that can be measured directly and r be the number of inputs. Then state space model is defined as shown below.

$$\begin{aligned} \dot{X} &= AX + BU \\ Y &= HX + DU \end{aligned} \qquad (3.1)$$

Where, X is a $n \times 1$ state space vector

Y is a $p \times 1$ measurement vector

U is a $r \times 1$ input vector

A is a $n \times n$ matrix characterizing the state vector evolution in time

B is a $n \times r$ matrix characterizing the relation between state and input vectors

H is a $p \times n$ matrix characterizing the relation between output and state vectors

D is a $p \times r$ matrix characterizing the relation between output and input vectors

Output measured from a system with no input applied to it, is called the natural response of system. State space model of a system which do not have inputs is given by equation (3.2).

$$\begin{aligned} \dot{X} &= AX \\ Y &= HX \end{aligned} \qquad (3.2)$$

In general, measurements obtained are not the actual values but a noise corrupted version. Measurement errors arise because of irregularities in the measuring devices and uncertainties in modeling the system. Models are developed based on the behavior of large amounts of data in a particular scenario; hence it is a good approximation to characterize the difference in observations and the model predicted values, as zero mean Gaussian random variable (Central Limit Theorem). Therefore, process noise in the state dynamic equation is characterized by a zero mean Gaussian random vector with covariance say Q. Measurement errors can also be characterized along the same lines and hence measurement noise is a zero mean Gaussian random vector with covariance denoted by R. In order to accommodate the terms characterizing randomness of state space equations model described by equation (3.2) has to be modified as in (3.3).

$$\begin{aligned} \dot{X} &= AX + w \\ Y &= HX + v \end{aligned} \quad (3.3)$$

Where, w is a $n \times 1$ process noise vector

v is a $p \times 1$ measurement noise vector

The state space model described in equation (3.1) is only applicable for linear systems. A more generalized way of describing the state space is given by equation (3.4).

$$\begin{aligned} X_k &= f(X_{k-1}, w_{k-1}) \\ Z_k &= h(X_k, v_k) \end{aligned} \quad (3.4)$$

Where X_{k-1}, w_{k-1} denote the state vector and process noise at time $k-1$, X_k is the state vector at time k, Z_k and v_k are the measurement and noise at time k.

3.1.1 State space model for localization

State Dynamic Equation

$$X_k = X_{k-1} + w_{k-1} \qquad (3.5)$$

Measurement Equation

$$Z_k = C_1 - C_2 \log\left(\left(X_k - Y_k\right)^T \left(X_k - Y_k\right)\right) + v_k \qquad (3.6)$$

Where C_1 and C_2 are constants depending on the path loss model. Y_k and Z_k are the measured position and power vectors.

3.2 Nonlinear Bayesian Estimation

Bayesian state estimation aims to construct the conditional probability $P(X_k \mid Z_{1:k})$ also known as posterior density. Assuming that $P(X_0 \mid Z_0)$ is available at time $k = 0$, recursive steps of prediction and update of Bayesian estimator are given by equations (3.7) and (3.9) and are depicted in figure 9. Figure 10 depicts the flow chart for Bayesian estimation.

Prediction

In this step, state vector at time k is predicted using Chapman-Kolmogorov equation as given by equation (3.7).

$$P(X_k \mid Z_{1:k-1}) = \int_{X_{k-1}} P(X_k \mid X_{k-1}) P(X_{k-1} \mid Z_{1:k-1}) dX_{k-1} \qquad (3.7)$$

$P(X_k \mid X_{k-1})$ also known as Prior density, is dependent on the state vector at time $k-1$ and state dynamic equation. $P(X_{k-1} \mid Z_{1:k-1})$ is the posterior probability density at time $k-1$.

Update

Posterior density of state vector at time k is computed in this phase. It is dependent on predicted density $P(X_k \mid Z_{1:k-1})$, computed in the earlier step and measurement model. Recursive method for computing posterior density is derived as shown below.

$$P(X_k \mid Z_{1:k}) = \frac{P(X_k, Z_{1:k})}{P(Z_{1:k})} \qquad (3.8)$$

Applying Bayes rule,

$$P(X_k \mid Z_{1:k}) = \frac{P(Z_k, Z_{1:k-1} \mid X_k) P(X_k)}{P(Z_k, Z_{1:k-1})}$$

$$P(X_k \mid Z_{1:k}) = \frac{P(Z_k \mid Z_{1:k-1}, X_k) P(Z_{1:k-1} \mid X_k) P(X_k)}{P(Z_k \mid Z_{1:k-1}) P(Z_{1:k-1})}$$

Applying Bayes rule again,

$$P(X_k \mid Z_{1:k}) = \frac{P(Z_k \mid Z_{1:k-1}, X_k) P(X_k \mid Z_{1:k-1}) P(Z_{1:k-1})}{P(Z_k \mid Z_{1:k-1}) P(Z_{1:k-1})}$$

Using the independence of measurements,

$$P(X_k \mid Z_{1:k}) = \frac{P(Z_k \mid X_k)P(X_k \mid Z_{1:k-1})}{P(Z_k \mid Z_{1:k-1})}$$

$$P(X_k \mid Z_{1:k}) = \frac{P(Z_k \mid X_k)P(X_k \mid Z_{1:k-1})}{\int_{X_k} P(Z_k \mid X_k)P(X_k \mid Z_{1:k-1})dX_k} \qquad (3.9)$$

$P(Z_k \mid X_k)$ also called as likelihood, is determined using the measurement model. Although above recursive steps of prediction and update constitute the optimal solution of Bayesian estimation, in general it does not guarantee a closed form solution.

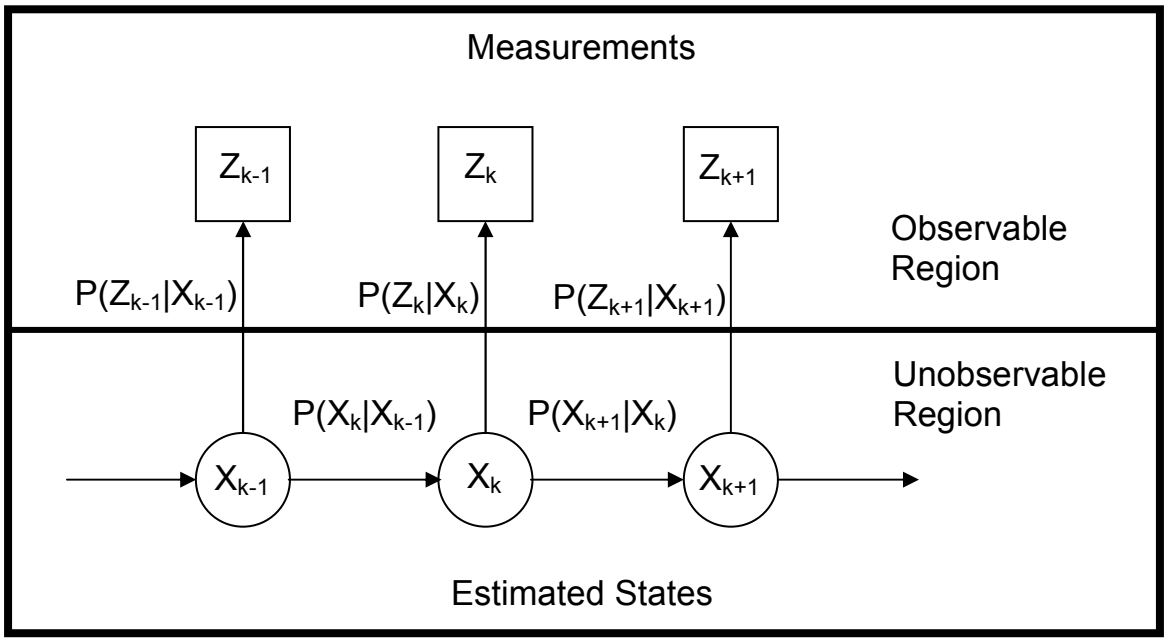

Figure 9 : Evolution of Bayesian State Estimation with time

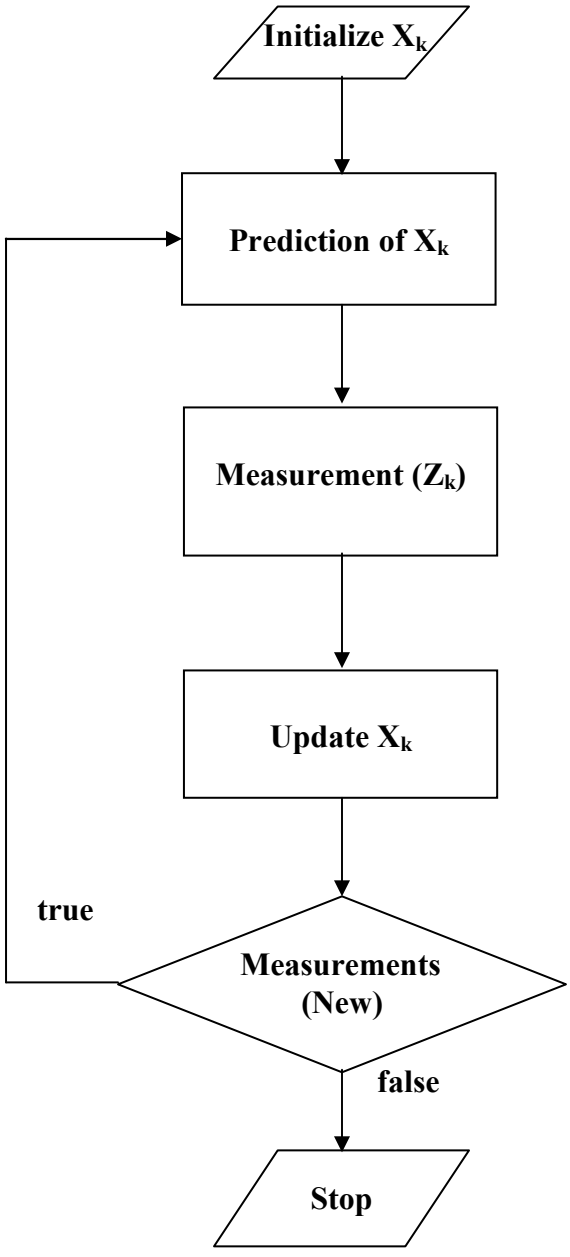

Figure 10 : Flow chart for Bayesian State Estimation

3.2.1 Recursive Bayesian estimation for localization

Recursive Bayesian estimation consists of prediction and update phases as described below. In the first phase, the state probability is predicted using state dynamic equation which will be updated using current measurements in the later phase.

Prediction Phase

Using the state dynamic equation, prior can be obtained as given by equation (3.11).

$$X_k = X_{k-1} + w_{k-1} \qquad (3.10)$$

$$P(X_k \le x_k) = P(X_{k-1} + w_{k-1} \le x_k) = P(w_{k-1} \le x_k - X_{k-1})$$

$$\Rightarrow P(X_k \le x_k \mid X_{k-1}) = P(w_{k-1} \le x_k - X_{k-1} \mid X_{k-1}) = P(w_{k-1} \le x_k - x_{k-1})$$

$$\Rightarrow P(w_{k-1} \le x_k - x_{k-1}) = F_w(x_k - x_{k-1})$$

$$\therefore P(X_k \mid X_{k-1}) = P_w(X_k - X_{k-1} \mid X_{k-1}) \qquad (3.11)$$

Predicted probability density of state is now computed as

$$P(X_k \mid Z_{1:k-1}) = \int_{-\infty}^{\infty} P_w(X_k - X_{k-1} \mid X_{k-1}) P(X_{k-1} \mid Z_{1:k-1}) dX_{k-1} \qquad (3.12)$$

As mentioned earlier, $P_w(w)$ follows Gaussian distribution and $P(X_{k-1} \mid Z_{1:k-1})$ is the posterior distribution obtained from previous recursion.

Update Phase

Two cases arise depending on the nature of locations' measurements.

1. Perfect knowledge of measured position coordinates.
2. Position coordinates follow a probability distribution.

Case 1: *Perfect knowledge of measured position coordinates*

Using the measurement model, likelihood probability is computed using equation (3.9).

$$P(Z_k \mid X_k) = P_w\left(Z_k - C_1 - C_2 \log\left((Y_k - X_k)^T (Y_k - X_k)\right) \mid X_k\right) \quad (3.13)$$

Posterior density is now computed as

$$P(X_k \mid Z_{1:k}) = \frac{P_w\left(Z_k - C_1 - C_2 \log\left((Y_k - X_k)^T (Y_k - X_k)\right) \mid X_k\right) P(X_k \mid Z_{1:k-1})}{\int_{-\infty}^{\infty} P_w\left(Z_k - C_1 - C_2 \log\left((Y_k - X_k)^T (Y_k - X_k)\right) \mid X_k\right) P(X_k \mid Z_{1:k-1}) dX_k} \quad (3.14)$$

Case 2: *Position coordinates follow a probability distribution*

For this case equation (3.13) is modified as given in (3.15).

$$P(Z_k \mid X_k) = \int_{-\infty}^{\infty} P_w\left(Z_k - C_1 - C_2 \log\left((Y_k - X_k)^T (Y_k - X_k)\right) \mid X_k, Y_k\right) P(Y_k) dY_k \quad (3.15)$$

Therefore, the posterior distribution is computed as

$$P(X_k \mid Z_{1:k}) = \frac{\left(\int_{-\infty}^{\infty} P_v\left(Z_k - C_1 - C_2 \log\left((Y_k - X_k)^T (Y_k - X_k)\right) \mid X_k, Y_k\right) P_{X_{1K}} dY_k\right) P(X_k \mid Z_{1:k-1})}{\int_{-\infty}^{\infty} \left(\int_{-\infty}^{\infty} P_v\left(Z_k - C_1 - C_2 \log\left((Y_k - X_k)^T (Y_k - X_k)\right) \mid X_k, Y_k\right) P_{X_{1K}} dY_k\right) P(X_k \mid Z_{1:k-1}) dX_k} \quad (3.16)$$

Where $P_v(v)$ is assumed to follow normal distribution with mean μ_v and variance σ_v, $P_{Y_k}(y_k)$ for simplicity, is also assumed to follow normal distribution with mean μ_{Y_k} and variance σ_{Y_k}.

3.2.2 Need for approximation

In equation (3.16), the integral in denominator does not have closed form solution. It is evident from the above equations that optimal analytical solution is not tractable for Localization and hence the need for approximation arises. There are many approximation strategies developed in literature that can provide sub-optimal solutions. There are two types of models for which the optimal solution exists, one assumes linear systems with Gaussian state and noise vectors and application of Kalman Filter. Other model assumes discrete state space with application of Grid based filters. Therefore, in order to obtain sub-optimal solutions for a given nonlinear continuous state space model, approximations can be made to the model. One way of doing approximation is by linearizing the model and approximating the state vector with a Gaussian random vector. Extended Kalman Filter makes use of this approximation and is widely applied in engineering applications. Chapter 4 examines the behavior of this filter for the localization application. One more possibility is by approximating the probability density by a set of point masses called sigma points, which accurately characterize the Gaussian distribution and then apply nonlinear operations on them. This solution is found to give better results than the earlier approximation for the cases where state vector is normally distributed and is called

Unscented Kalman Filter. Also, one can approximate the continuous state space with a discrete one and then apply Grid based filters.

Although above techniques may give acceptable results in applications where approximations are valid, they fail to provide a solution which can be applicable for any generalized state space model. One method which can make Bayesian estimation applicable for any system approximates the probability density by a set of particles with associated weights. 'Numerical Integration' and 'Monte Carlo methods' are the most widely used approximation techniques. Numerical Integration provides good accuracy but suffers from high computational requirement as the dimensionality of state vector increases. The number of operations to be performed increases exponentially with dimensions and hence is not advisable for higher dimensional systems. This limitation of numerical integration is also called as 'Curse of Dimensionality'. Monte Carlo methods can be employed to overcome the above mentioned drawbacks, which do not suffer from dimensions of the system. Sequential Monte Carlo method is one such approximation technique where the state posterior density is computed recursively based on Monte Carlo methods and will be dealt more detailed in chapter 5.

4. LOCALIZATION USING EXTENDED KALMAN FILTERING

This Chapter deals with the application of Extended Kalman Filtering (EKF) for Localization problem. As described in the previous chapter that a probabilistic solution is more meaningful than a deterministic one, EKF estimates the state probability density function conditioned on measurements by applying Kalman Filtering (KF). Direct application of KF is not possible because of the nonlinear state space model of localization and also the non-Gaussian nature of conditional state probability density function. In order to apply KF, approximations have to be made in the state space model as well as probability distribution which will be discussed shortly. Following section provides a brief review of KF and will be followed by a section dealing with system model for localization and finally application of EKF is presented along with simulation results.

4.1 Review of Kalman Filtering

Kalman Filtering (KF) is one of the most widely used algorithms in engineering applications. It gained prominence because of its guaranteed optimal solution apart from the simplicity in implementation. KF deals with the estimation of system states using available measurements and a predefined state space model iteratively. Following section reviews the KF analysis.

Using the state space model defined in equation (3.3), process noise of state dynamic equation is characterized by a zero mean Gaussian random vector with covariance say Q. Measurement errors can also be characterized along the same lines and let its covariance be denoted by R. The objective of KF is to design an estimator which can minimize some function of error e_k in estimating the state vector at time k based on observation Y_k. Let X_k and $\hat{X}_k$ be the true and estimated state vectors at time k, then the error is given as

$$e_k = X_k - \hat{X}_k \qquad (4.1)$$

Shape of the function of e_k is dependent on application but, the function has to be both positive and increase monotonically. An error function satisfying the above requirements is a squared error function

$$f(\underset{\hat{X}}{e_k}) = \left(X_k - \hat{X}_k\right)^2 \qquad (4.2)$$

As the vector $\hat{X}_k$ is estimated using the measurement data over time, a meaningful metric would be an expected value of the mean squared error function.

$$E\left\{\left(X_k - \hat{X}_k\right)^2\right\} = E\left\{\left(X_k - \hat{X}_k\right)^T\left(X_k - \hat{X}_k\right)\right\} = E\left\{e_k{}^T e_k\right\} = P_k \qquad (4.3)$$

Where P_k is the error covariance matrix.

Let $\hat{X}_k^-$ be the prior estimate of state vector obtained using prediction from system dynamics. If a measurement is available, then the state vector can be updated using the relation in equation (4.4).

$$\hat{X}_k = \hat{X}_k^- + K_k\left(Y_k - H\hat{X}_k^-\right) \qquad (4.4)$$

Where, the term $Y_k - H\hat{X}_k^-$ is called innovation and K_k, the Kalman gain.

Using the measurement equation of state space model and replacing Y_k in the above equation will result in equation (4.5).

$$\hat{X}_k = \hat{X}_k^- + K_k\left(HX_k + v_k - H\hat{X}_k^-\right) \quad (4.5)$$

Substituting the above equation in error covariance equation (4.3),

$$E\left\{\left(X_k - \hat{X}_k\right)^T\left(X_k - \hat{X}_k\right)\right\} = E\begin{bmatrix}\left\{\left(I - H\hat{X}_k^-\right)\left(X_k - \hat{X}_k^-\right) - K_k v_k\right\}\times \\ \left\{\left(I - H\hat{X}_k^-\right)\left(X_k - \hat{X}_k^-\right) - K_k v_k\right\}^T\end{bmatrix} \quad (4.6)$$

Where, $\left(X_k - \hat{X}_k^-\right)$ is the error of prior estimate and is uncorrelated with the measurement error v_k. Hence the above error covariance matrix is given as

$$P_k = \left(I - H\hat{X}_k^-\right)E\left[\left(X_k - \hat{X}_k^-\right)\left(X_k - \hat{X}_k^-\right)^T\right]\left(I - H\hat{X}_k^-\right)^T + K_k E\left[v_k {v_k}^T\right]{K_k}^T \quad (4.7)$$

$$P_k = \left(I - H\hat{X}_k^-\right)P_k^-\left(I - H\hat{X}_k^-\right)^T + K_k R {K_k}^T \quad (4.8)$$

Where P_k^- is the covariance of error in prior estimate $\hat{X}_k - \hat{X}_k^-$, and R is the covariance matrix of measurement noise vector.

Equation (4.8) defines the update of error covariance matrix which has mean squared error terms as its diagonal elements. Sum of the diagonal elements in a matrix is called trace. Therefore, trace of the error covariance matrix is the sum of mean squared errors and it can be minimized by minimizing the trace of the error covariance matrix.

Therefore, one needs to find a value of K_k that minimizes the trace of error covariance matrix. Using calculus, K_k should satisfy the condition of $\frac{\partial}{\partial K_k}\left[Trace(P_k)\right]=0$.

Expanding the error covariance matrix equation (4.8)

$$P_k = P_k^- - K_k H P_k^- - P_k^- H^T K_k^T + K_k\left(H P_k^- H^T + R\right)K_k^T \qquad (4.9)$$

Trace of the error covariance can be obtained by the following equation. Note that the trace of a matrix and its transpose are equal.

$$T\left[P_k\right] = T\left[P_k^-\right] - 2T\left[K_k H P_k^-\right] + T\left[K_k\left(H P_k^- H^T + R\right)K_k^T\right] \qquad (4.10)$$

Differentiating the above equation with respect to K_k and equating it to zero, we get

$$\frac{\partial T(P_k)}{\partial K_k} = 0 = -2\left(H P_k^-\right)^T + 2K_k\left(H P_k^- H^T + R\right) \qquad (4.11)$$

$$K_k = P_k^- H^T\left(H P_k^- H^T + R\right)^{-1} \quad (4.12)$$

Above equation gives the update of gain matrix and substituting it in error covariance equation, we get

$$P_k = P_k^- - P_k^- H^T\left(H P_k^- H^T + R\right)^{-1} H P_k^- \qquad (4.13)$$

$$P_k = \left(I - K_k H\right)P_k^- \qquad (4.14)$$

Equation (4.14) is the update equation for error covariance matrix. Thus, one can obtain the update equations for state vector, Kalman gain and error covariance matrix as given by equations (4.5), (4.12) and (4.14) respectively. After updating aforementioned

quantities for the k^{th} iteration based on prior estimates, state vector and its error covariance for the next iteration has to be predicted. State dynamic equation describing the time evolution of system is used for prediction. Therefore, prior estimate for the next iteration is computed as

$$\hat{X}_{k+1}^{-} = A\hat{X}_k \quad (4.15)$$

And the covariance of error in prior estimate is computed as shown below

$$P_{k+1}^{-} = E\left[\left(e_{k+1}^{-}\right)^T e_{k+1}^{-}\right] \qquad (4.16)$$

Where, $e_{k+1}^{-} = X_{k+1} - \hat{X}_{k+1}^{-} = AX_k + w_k - A\hat{X}_k = Ae_k + w_k$

$$P_{k+1}^{-} = E\left[\left(Ae_k + w_k\right)^T \left(Ae_k + w_k\right)\right] \qquad (4.17)$$

Error vector e_k and noise vector w_k are uncorrelated because of different sources of origin. Hence, equation for error covariance of prior estimate at k^{th} iteration is given as in (4.19).

$$P_{k+1}^{-} = A^T E\left[e_k^{\ T} e_k\right] A + E\left[w_k^{\ T} w_k\right] \qquad (4.18)$$

$$P_{k+1}^{-} = A^T P_k A + Q \qquad (4.19)$$

This equation completes the prediction phase. Update phase and prediction phase together constitute an iteration of the Kalman filter. Filter equations are summarized as shown below.

4.1.1 Steps in Kalman Filter

Initialization

Initialize the state vector with X_0 and error covariance matrix P_0 with arbitrary large values in its diagonal elements and rest all set to zero.

Update Phase

Gain update

$$K_k = P_k^{-} H^T \left(H P_k^{-} H^T + R \right)^{-1} \quad (4.20)$$

State update

$$\hat{X}_k = \hat{X}_k^{-} + K_k \left(Y_k - H \hat{X}_k^{-} \right) \quad (4.21)$$

Error covariance update

$$P_k = \left(I - K_k H \right) P_k^{-} \quad (4.22)$$

Prediction Phase

State prediction

$$\hat{X}_{k+1}^{-} = A \hat{X}_k \quad (4.23)$$

Error Covariance prediction

$$P_{k+1}^{-} = A^T P_k A + Q \quad (4.24)$$

4.2 System Model for Localization

State Dynamic Model

$$\begin{bmatrix} x_{k+1} \\ y_{k+1} \\ z_{k+1} \end{bmatrix} = \begin{bmatrix} x_k \\ y_k \\ z_k \end{bmatrix} + \begin{bmatrix} w_{kx} \\ w_{ky} \\ w_{kz} \end{bmatrix} \qquad (4.25)$$

Measurement Model

$$\begin{bmatrix} P_{r1} \\ P_{r2} \\ P_{r3} \end{bmatrix} = \begin{bmatrix} P_t + G_t + G_r - L_p(d_{01}) \\ P_t + G_t + G_r - L_p(d_{02}) \\ P_t + G_t + G_r - L_p(d_{03}) \end{bmatrix} \qquad (4.26)$$

Replacing $L_p(d_0)$ with $L_p(d_{00}) + 10\eta \log_{10}(d_0)$, the measurement model is modified as

$$\begin{bmatrix} P_{r1} \\ P_{r2} \\ P_{r3} \end{bmatrix} = \begin{bmatrix} P_t + G_t + G_r - L_p(d_{00}) - 10\eta \log_{10}(d_{01}) \\ P_t + G_t + G_r - L_p(d_{00}) - 10\eta \log_{10}(d_{02}) \\ P_t + G_t + G_r - L_p(d_{00}) - 10\eta \log_{10}(d_{03}) \end{bmatrix} + \begin{bmatrix} v_1 \\ v_2 \\ v_3 \end{bmatrix} \qquad (4.27)$$

Vectors w and v are the state and measurement noises distributed as zero mean Gaussian random variables with covariance matrices Q and R respectively. Substituting the value of d_{0i} as a function of measurement and target (state vector) locations in the measurement equations, measurement vector in terms of state vector is represented as in equation (4.28). Where K is a constant term used to replace the terms $P_t + G_t + G_r - L_p(d_{00})$.

$$\begin{bmatrix} P_{r1k} \\ P_{r2k} \\ P_{r3k} \end{bmatrix} = \begin{bmatrix} K - 10\eta \log_{10}(\sqrt{(x-x_{1k})^2 + (y-y_{1k})^2 + (z-z_{1k})^2}) \\ K - 10\eta \log_{10}(\sqrt{(x-x_{2k})^2 + (y-y_{2k})^2 + (z-z_{2k})^2}) \\ K - 10\eta \log_{10}(\sqrt{(x-x_{3k})^2 + (y-y_{3k})^2 + (z-z_{3k})^2}) \end{bmatrix} + \begin{bmatrix} v_{1k} \\ v_{2k} \\ v_{3k} \end{bmatrix} \quad (4.28)$$

Observing the measurement model of system designed for localization, it is evident that direct application of Kalman Filter is not possible. As the measurement vector is a nonlinear function of the state vector, the filter has to be modified such that measurement can be linearized about its current mean and covariance. Hence it is appropriate to use an approximation of the Kalman Filter namely Extended Kalman Filter which extends the application of Kalman filter to nonlinear dynamic systems.

4.3 Extended Kalman Filtering

Extended Kalman filtering is applicable for nonlinear systems because of the approximation of state space model using Taylor's series expansion and neglecting higher order terms. State space model for the nonlinear systems assuming zero input vector can be represented as shown below.

State Model

$$X_{k+1} = f\left(\hat{X}_k, w_k\right) \quad (4.29)$$

Measurement Model

$$Z_{k+1} = h\left(\hat{X}_{k+1}, v_{k+1}\right) \quad (4.30)$$

As one does not have prior knowledge about the value of w_k and v_k, estimate of the sate and measurement vectors are computed with above noises set to zero. The modified model is as shown below

State Model

$$\hat{X}_{k+1} = f\left(\hat{X}_k, 0\right) \qquad (4.31)$$

Measurement Model

$$Z_{k+1} = h\left(\hat{X}_{k+1}, 0\right) \qquad (4.32)$$

State update and prediction equations for the above system are given below

Update Phase

Gain update

$$K_k = P_k^{-} H^{*}\left(HP_k^{-} H^{*} + VRV^{*}\right)^{-1} \qquad (4.33)$$

State update

$$\hat{X}_k = \hat{X}_k^{-} + K_k\left(Y_k - H\hat{X}_k^{-}\right) \qquad (4.34)$$

Error covariance update

$$P_k = \left(I - K_k H\right)P_k^{-} \qquad (4.35)$$

Prediction Phase

State prediction

$$\hat{X}_{k+1}^{-} = A\hat{X}_k \qquad (4.36)$$

Error Covariance prediction

$$P_{k+1}^{-} = A^T P_k A + WQW^T \qquad (4.37)$$

Where the matrices A, H, W and V are Jacobians defined as

$$A(i,j) = \frac{\partial f_i}{\partial x_j}(\hat{X}_{k-1},0) \qquad (4.38)$$

$$H(i,j) = \frac{\partial h_i}{\partial x_j}(\hat{X}_k,0) \qquad (4.39)$$

$$W(i,j) = \frac{\partial f_i}{\partial w_j}(\hat{X}_{k-1},0) \qquad (4.40)$$

$$V(i,j) = \frac{\partial f_i}{\partial v_j}(\hat{X}_k,0) \qquad (4.41)$$

Flow chart depicted in figure 10 for Bayesian estimation is applicable for Kalman and Extended Kalman filters as well. Prediction and update steps are implemented as depicted in figure 11. Matrices involved in Extended Kalman filter have to be calculated recursively as given in equations (4.38) – (4.41) and

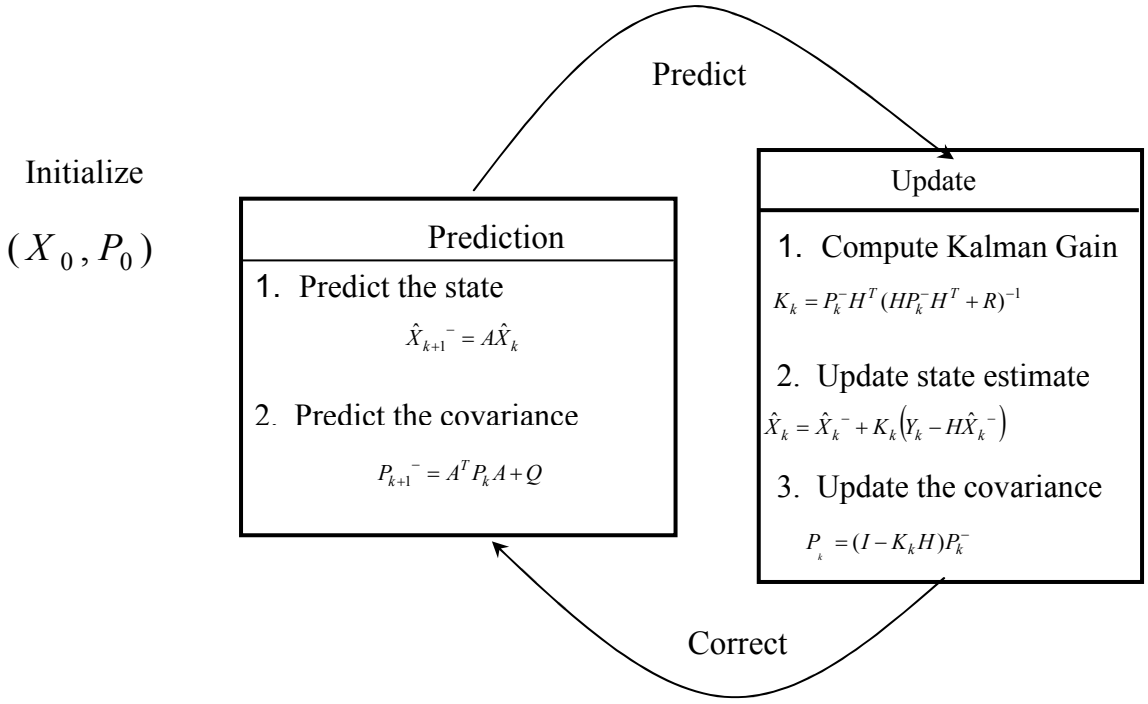

Figure 11 : Flow chart for Bayesian State Estimation

4.3.1 Localization model for EKF

System model for the localization application was introduced in section 3.2 for Kalman Filter. Applying the Extended Kalman Filter for localization model, state prediction stage remains the same as the state dynamic equation is linear, but the state update equations get modified because of the linearization process, as given in the Extended Kalman Filter state update phase. Matrix H is derived as shown below.

$$H(i,j) = \frac{\partial h_i}{\partial x_j}(\hat{X}_k, 0) \quad (4.42)$$

Where h is the measurement function in equation (4.32) and its Jacobian is computed to be

$$H = 10\eta \begin{bmatrix} \frac{x_1 - x}{d_1} & \frac{y_1 - y}{d_1} & \frac{z_1 - z}{d_1} \\ \frac{x_2 - x}{d_2} & \frac{y_2 - y}{d_2} & \frac{z_2 - z}{d_2} \\ \frac{x_3 - x}{d_3} & \frac{y_3 - y}{d_3} & \frac{z_3 - z}{d_3} \end{bmatrix} \quad (4.43)$$

Matrices A, Q and R are identity matrices of order 3×3 as they are linearly related to state and measurement vectors. Simulation results for the extended Kalman Filter are demonstrated in the following section with figures 12 - 15.

4.4 Simulation Results

This section presents the simulation results of the EKF. Parameters for the simulation are given below.

Path loss exponent $\eta = 4$

Standard deviation of process noise $\sigma_2 = 1$ meter

Standard deviation of measurement noise (Shadowing) $\sigma_1 = 6dB$

Standard deviation of location measurements $\sigma_3 = 5$ meters

Number of locations $= 25$

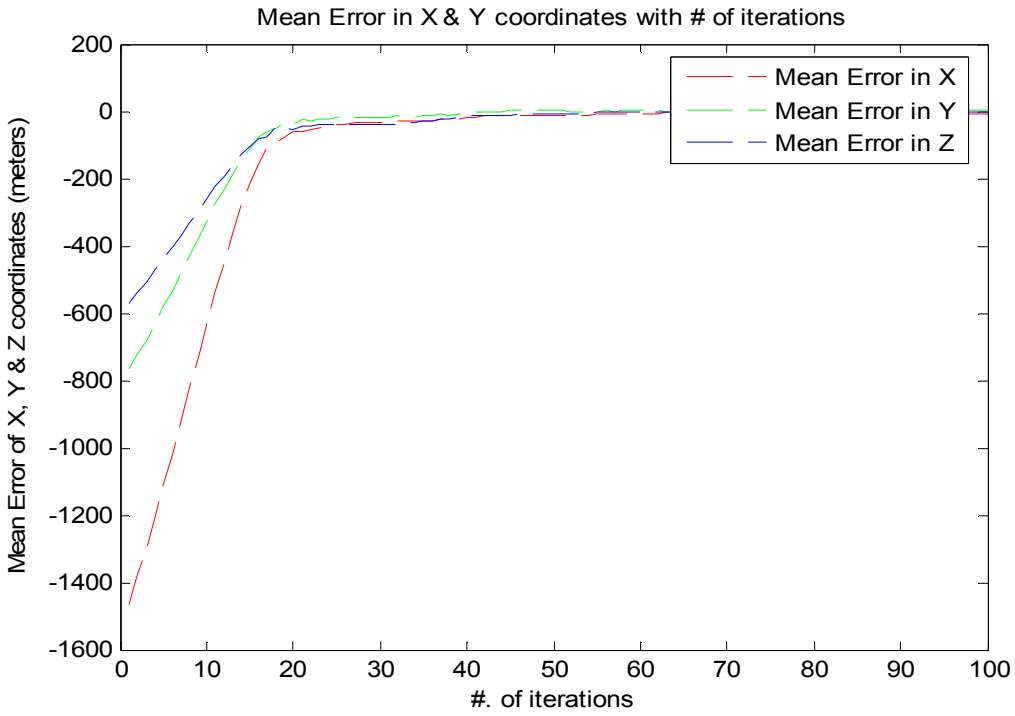

Figure 12 : Plot of EKF Mean Error in coordinates vs. Time

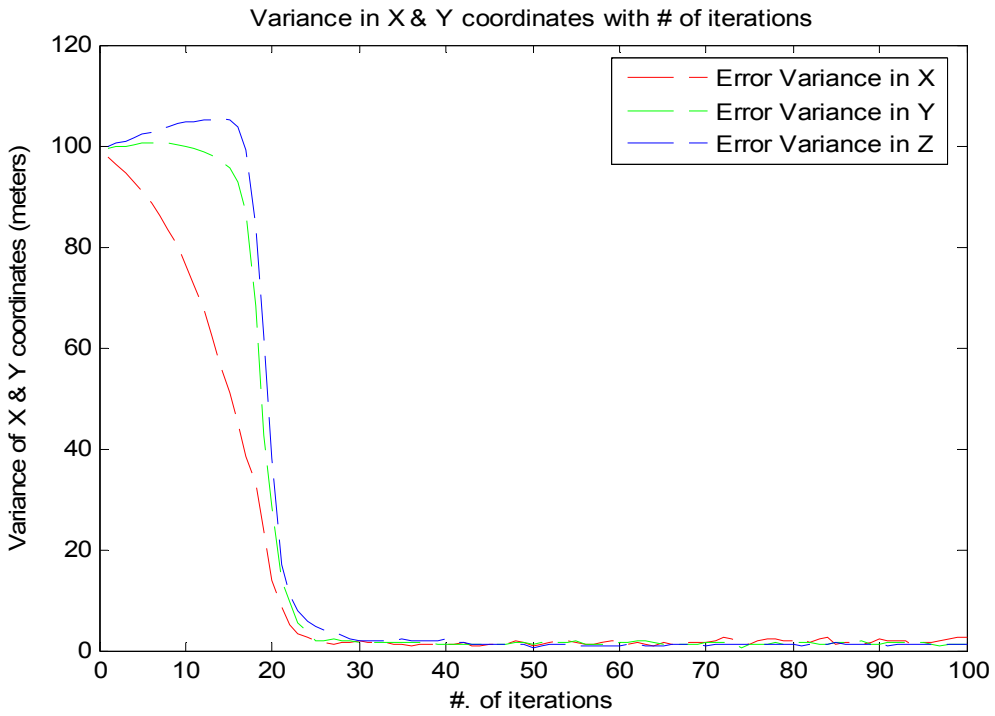

Figure 13 : Plot of EKF Error Variance in coordinates vs. Time

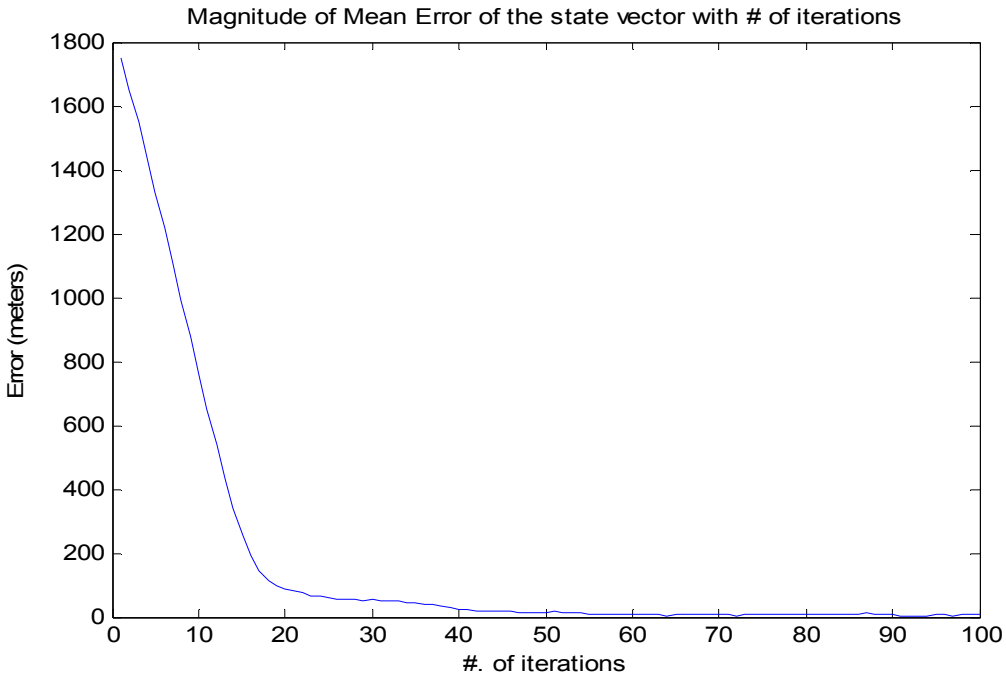

Figure 14 : Plot of EKF Mean Error vs. Time

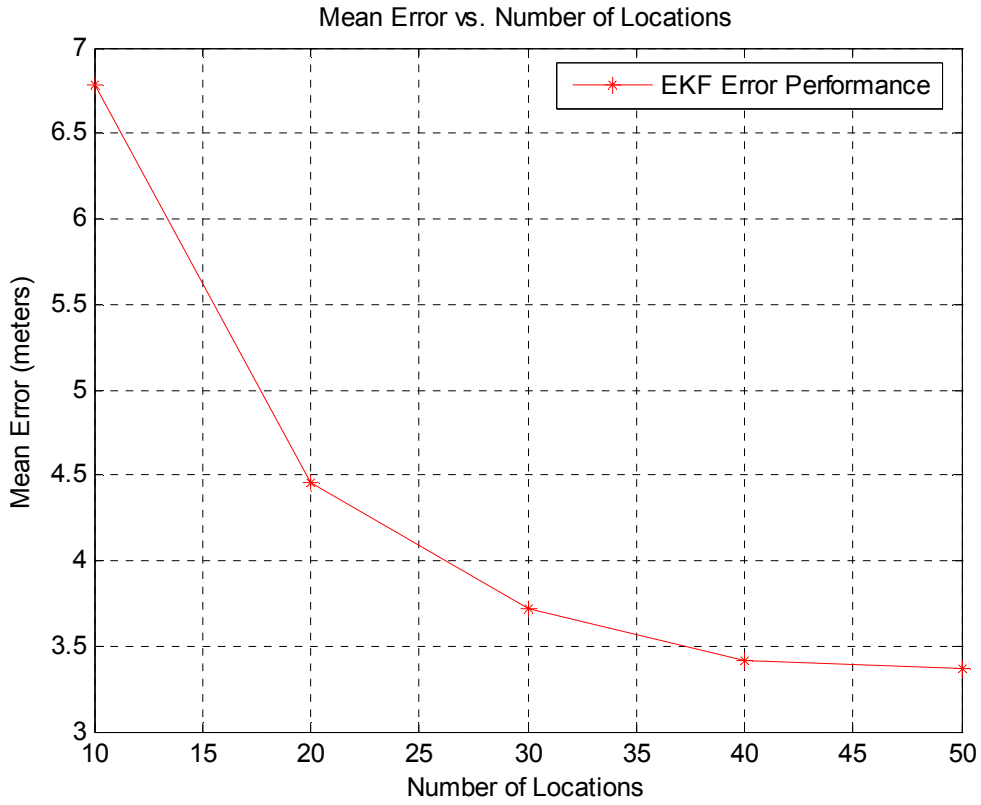

Figure 15 : Plot of EKF Mean Error vs. Number of Locations

Error performance of the Extended Kalman Filter as function of Number of locations is given in figure 15. All the parameters are same as that mentioned above except for number of locations. For each location, the error is averaged after performing simulations for 100 times and is so chosen that average error does not vary much with further increase in number of simulations.

Error is computed as the difference between estimated mean and actual location. From figure 14, it can be inferred that, as the number of measurement locations increase, the

error decreases. This is because of the obvious reason that effect of shadowing will be negated. Although EKF provides acceptable results considering the error with respect to its mean, this filter limits the amount of knowledge conveyed about actual state probability distribution because of Gaussian approximation. As the Gaussian distribution is characterized by its mean and Covariance, using this filter, one can only estimate the first and second order moments of state posterior density. In order to get more information like higher order moments, quantiles about the distribution of location coordinates, Gaussian assumption has to be eliminated and a more generalized approach has to be applied.

4.5 Comparison of RLSF and EKF

For a given path loss model and target location, RLSF and EKF are simulated for 100 times and the average error has been computed for each of the measurement locations. i.e. [10:10:50]. Figure 16 provides the average error performance of RLSF and EKF. The performance of later algorithm is observed to be superior to that of former.

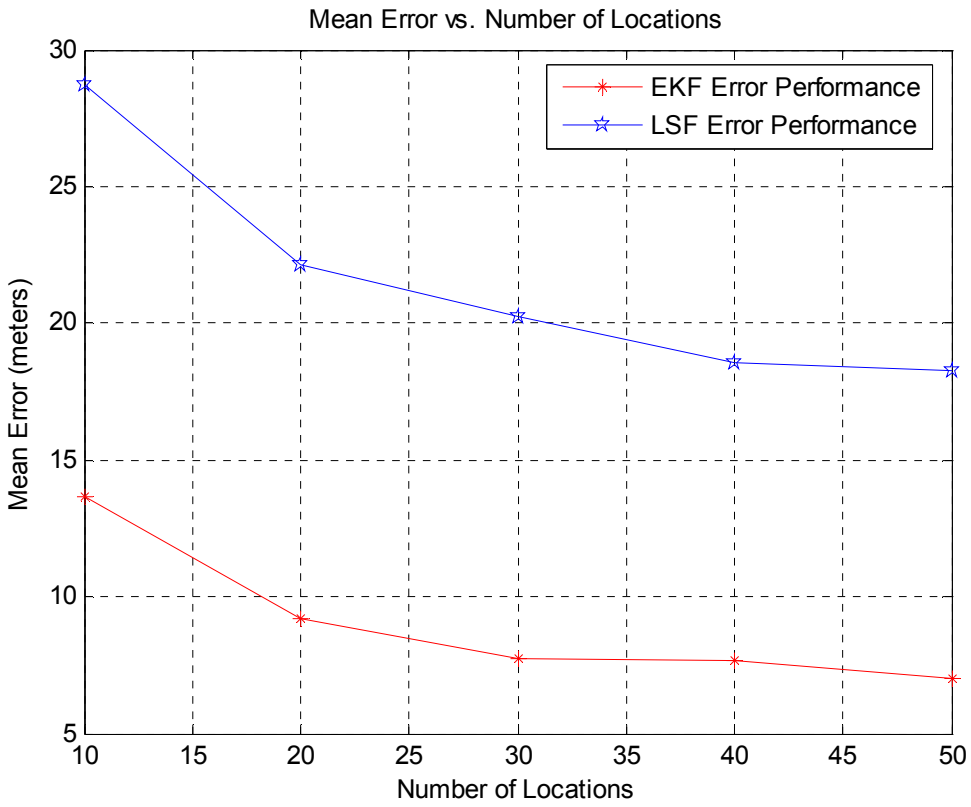

Figure 16 : Comparison of EKF and RLSF Mean error performance

5. MONTE CARLO METHODS AND PARTICLE FILTER

5.1 Monte Carlo methods

As the analytical solution is not tractable for localization problem, Monte Carlo approximation has been employed for building the posterior density function. Monte Carlo methods are a class of algorithms which require repeated random sampling to compute estimates. This section gives a brief introduction about Monte Carlo methods and importance sampling. These methods are used to compute expectations of complex probability functions using a set of independent and identically distributed random samples drawn from the probability distribution. Following example illustrates the method of approximation using Monte Carlo. Suppose X is a random variable with probability density function $P_X(x)$, then an expectation of function of X, $f(X)$ can be computed as

$$\widetilde{f}(X) = E_P[f(X)] = \frac{1}{Ns}\left[\sum_{i=1}^{Ns} f\left(X^{(i)}\right)\right] \qquad (5.1)$$

Where $X^{(i)}$ are independent random samples drawn from Ω, the sample space of X according to the probability density function $P_X(x)$. $\widetilde{f}(X)$ is called the Monte Carlo Estimator for expectation of $f(X)$.

Monte Carlo methods make use of "law of large numbers" to prove that, as the number of samples used for estimation gets large, approximated estimate approaches the original estimate, if it exists. Law of Large Numbers states that average of a large number of independent random samples from a probability distribution tends towards the theoretical average of that distribution.

$$\lim_{Ns\to\infty} P\left(\left|\widetilde{f}_{Ns}(X) - E_P\left[f(X)\right]\right| \geq \varepsilon\right) = 0 \qquad (5.2)$$

Hence, if N_s is chosen to be large, then the probability that $\widetilde{f}(X)$ deviates from $E_P[f(X)]$ will be very small.

5.1.1 Mean and variance of Monte Carlo estimator

Let us consider the properties of Monte Carlo estimator $\widetilde{f}(X)$ as a random variable. The mean and variance of the estimate are computed as given by equations (5.3) and (5.4).

$$E\left[\widetilde{f}_{Ns}(X)\right] = E\left[\frac{1}{Ns}\sum_{i=1}^{Ns} f\left(X^{(i)}\right)\right] = \frac{1}{Ns}\sum_{i=1}^{Ns} E\left[f\left(X^{(i)}\right)\right] = E\left[f(X)\right] \qquad (5.3)$$

$$Var\left[\widetilde{f}(X)\right] = Var\left[\frac{1}{Ns}\sum_{i=1}^{Ns} f\left(X^{(i)}\right)\right] = \frac{1}{Ns^2}\sum_{i=1}^{Ns} Var\left[f\left(X^{(i)}\right)\right] = \frac{1}{Ns} Var\left[f(X)\right] \qquad (5.4)$$

One of the important aspects of Monte Carlo estimators is that they are unbiased and have a small variance if the number of samples tends to towards infinity. The estimator introduced here is also called as crude Monte Carlo. Numerous variance reduction

techniques have been developed in the literature among which "Importance Sampling" has been widely adopted.

5.1.2 Importance Sampling

Importance Sampling deals with choosing a good distribution from which it is easy to generate random samples for computing Monte Carlo (MC) estimates. Basically, the integrand in an expectation equation is multiplied and divided by a proposal density to compute expectation with respect to the proposal density function. Using this method, an expectation of a quantity that varies less than the original integrand over region of integration, can be computed. Let $\pi(X)$ be the probability density function of X also called as proposal density, which takes values in Ω, satisfying the condition of (5.5).

$$\int_{x\in\Omega} \pi(x)dx = 1 \qquad (5.5)$$

Expectation for function $f(X)$ with X having a probability density $P(X)$ also called as target density over the same region Ω, can be computed as given in (5.6) for the values of X such that $\pi(x) \neq 0$.

$$\int_{x\in\Omega} f(x)P(x)dx = \int_{x\in\Omega} f(x)P(x)\frac{\pi(x)}{\pi(x)}dx = \int_{x\in\Omega} f(x)\frac{P(x)}{\pi(x)}\pi(x)dx = E_{\pi}\left[\frac{f(x)P(x)}{\pi(x)}\right] \qquad (5.6)$$

Monte Carlo estimator can be obtained by drawing the i.i.d random samples from $\pi(x)$ and computing the summation.

$$\tilde{f}_{Ns}{}^{\pi}(X) = E_{\pi}\left[\frac{f(X)P(X)}{\pi(X)}\right] = \frac{1}{Ns}\left[\sum_{i=1}^{Ns} f\left(X^{(i)}\right)\frac{P\left(X^{(i)}\right)}{\pi\left(X^{(i)}\right)}\right] \tag{5.7}$$

The variance of MC estimator thus computed can be minimized by choosing a proposal density which satisfies the condition $\pi(X) \propto P(X)$. If the proposal density is chosen such that $\pi(X) = \alpha P(X)$, then the resulting variance of MC estimator will be zero. Therefore, in order to compute a MC estimate using importance sampling, one needs to have the knowledge of target density function in order to build a proposal density such that it satisfies the above condition for minimum variance. In the ideal case, proposal density can be chosen to be the posterior density such that the resultant variance becomes zero. But, in general, the target distributions are complex and difficult to draw samples from it and hence the need for proposal density construction arises. The main application of importance sampling arises in these situations where the proposal density is chosen such that it is easy to draw samples and also should closely approximate the target density. For state estimation using Monte Carlo methods with importance sampling called particle filters have been developed which will be described in the next chapter.

Particle filters are sequential Monte Carlo methods applying Bayesian estimation for a generalized state space model. They make use of discrete particles to represent probability density function. Particle filter does not impose any restrictions on the distribution of state vector or process and measurement noises as is the case with Kalman filters and its variants. Following section describes some of the algorithms developed for particle filtering employing importance sampling.

5.2 Sequential Importance Sampling Algorithm (SIS)

Sequential Monte Carlo method that provides basic framework for particle filters is the algorithm of Sequential Importance Sampling (SIS). This method is also called as bootstrap filtering, condensation algorithm, particle filtering, interacting particle approximations and survival of the fittest. SIS algorithm is designed for recursive Bayesian estimation using Monte Carlo Simulations. It essentially approximates a probability density function by a set of particles with associated weights and then performs the operations of prediction and update recursively to approximate the posterior density. After a sufficient number of iterations, the distribution of particles becomes stationary and Monte Carlo estimates can be computed. As the number of particles becomes large, closer will be the representation of particles to the original posterior density which in turn will result in better estimates.

5.2.1 Prerequisites of SIS

In order to implement the SIS algorithm, one needs to have a set of random samples $X_k^{(i)}$ and their weights $w_k^{(i)}$ where $i = 1,2,.....Ns$ at time k to approximate the posterior probability density given measurements as

$$P(X_{0:k} \mid Z_{1:k}) \approx \sum_{i=1}^{Ns} w_k^{(i)} \delta\left(X_{0:k} - X_{0:k}^{(i)}\right) \qquad (5.8)$$

which is a discrete approximation of the original posterior density. Weights $w_k^{(i)}$ are obtained using the importance sampling as it is generally difficult if not impossible to

draw samples from posterior density directly. Initially at time $k = 0$, the posterior distribution $P(X_0 \mid Z_0) = P(X_0)$ is assumed to be known and also have a state space model of the system such that state transition density $P(X_k \mid X_{k-1})$ and likelihood density $P(Z_k \mid X_k)$ are defined. Now, the purpose of particle filter is to recursively estimate the posterior density $P(X_k \mid Z_{1:k})$ based on a given set of observations $Z_{1:k}$. In order to compute the weights recursively to approximate the posterior density, $X_{0:k}^{(i)}$ has to be drawn from posterior density but as it is impossible to do so, importance sampling method using a proposal density has to be employed. The proposal density has to be chosen such that it closely approximates the posterior and on the other hand samples can be drawn with ease.

Let $\pi(X_{0:k} \mid Z_{1:k})$ be the proposal density from which the samples $X_k^{(i)}$ are drawn and the weights are computed as

$$w_k^{(i)} \propto \frac{P\left(X_{0:k}^{(i)} \mid Z_{1:k}\right)}{\pi\left(X_{0:k}^{(i)} \mid Z_{1:k}\right)} \qquad (5.9)$$

The optimal choice of importance density is $\pi\left(X_{0:k}^{(i)} \mid Z_{1:k}\right) = P\left(X_{0:k}^{(i)} \mid Z_{1:k}\right)$. In the sequential Monte Carlo case, for every iteration samples representing posterior $P(X_{0:k-1} \mid Z_{1:k-1})$ from previous iteration will be available and are required to compute $P(X_{0:k} \mid Z_{1:k})$ with a new set of samples. Suppose one chooses an importance density such that

$$\pi(X_{0:k} \mid Z_{1:k}) = \pi(X_0 \mid Z_0) \prod_{i=1}^{k} \pi(X_k \mid X_{0:k-1}, Z_{1:k}) \qquad (5.10)$$

then, one can obtain the samples $X_{0:k}^{(i)}$ from $\pi(X_{0:k} \mid Z_{1:k})$ by augmenting each of the existing samples $X_{0:k-1}^{(i)}$ from $\pi(X_{0:k-1} \mid Z_{1:k-1})$ with new state $X_k^{(i)}$ drawn from $\pi(X_k \mid X_{0:k-1}, Z_{1:k})$.

5.2.2 Recursive steps in SIS

Using recursive Bayesian filter equations of prediction and update, the weight of the particles are computed recursively as shown below.

Prediction

$$P(X_{0:k} \mid Z_{1:k-1}) = P(X_k \mid X_{0:k-1}) P(X_{0:k-1} \mid Z_{1:k-1}) \qquad (5.11)$$

Update

$$P(X_{0:k} \mid Z_{1:k}) = \frac{P(Z_k \mid X_k) P(X_{0:k} \mid Z_{1:k-1})}{P(Z_k \mid Z_{1:k-1})} \qquad (5.12)$$

These two equations can be combined to form a single recursive equation for computing the weights of particle as

$$P(X_{0:k} \mid Z_{1:k}) = \frac{P(Z_k \mid X_k) P(X_k \mid X_{0:k-1})}{P(Z_k \mid Z_{1:k-1})} P(X_{0:k-1} \mid Z_{1:k-1}) \qquad (5.13)$$

$$P(X_{0:k} \mid Z_{1:k}) \propto P(Z_k \mid X_k) P(X_k \mid X_{0:k-1}) P(X_{0:k-1} \mid Z_{1:k-1}) \qquad (5.14)$$

Particle weights are computed as

$$w_k^{(i)} \propto \frac{P\left(X_{0:k} \mid Z_{0:k}\right)}{\pi\left(X_{0:k} \mid Z_{1:k}\right)} \qquad (5.15)$$

Substituting the values of $P\left(X_{0:k} \mid Z_{0:k}\right)$ and $\pi\left(X_{0:k} \mid Z_{1:k}\right)$ from equations (5.1.7) and (5.10) respectively

$$w_k^{(i)} \propto \frac{P\left(X_k^{(i)} \mid X_{k-1}^{(i)}\right) P\left(Z_k \mid X_k^{(i)}\right) P\left(X_{0:k-1}^{(i)} \mid Z_{0:k-1}^{(i)}\right)}{\pi\left(X_k \mid X_{0:k-1}, Z_{1:k}\right) \pi\left(X_{0:k-1} \mid Z_{1:k-1}\right)} \qquad (5.16)$$

$$w_k^{(i)} = w_{k-1}^{(i)} \frac{P\left(X_k^{(i)} \mid X_{k-1}^{(i)}\right) P\left(Z_k \mid X_k^{(i)}\right)}{\pi\left(X_k \mid X_{0:k-1}, Z_{1:k}\right)} \qquad (5.17)$$

Where $w_{0:k}^{(i)}$ and $w_{0:k-1}^{(i)}$ are the weights representing posterior density at times k and $k-1$ respectively. Once the weights are computed, then the posterior density can be represented by equation (5.8). Flow chart of the SIS algorithm is depicted in figure 17.

5.2.3 Pseudo Code for SIS Algorithm

1. Initialize by sampling particles from $P(X_0 \mid Z_0)$ at $k = 0$.
2. Iterate steps 3 to 5 for every k.
3. Draw samples at k using proposal density $\pi\left(X_k \mid X_{0:k-1}, Z_{1:k}\right)$.
4. Compute weights $\tilde{w}_k$ using equation (5.17).
5. Normalize particle weights as $w_k^{\,i} = \frac{\tilde{w}_k^{\,i}}{\sum_{i=1}^{Ns} \tilde{w}_k^{\,i}}$.

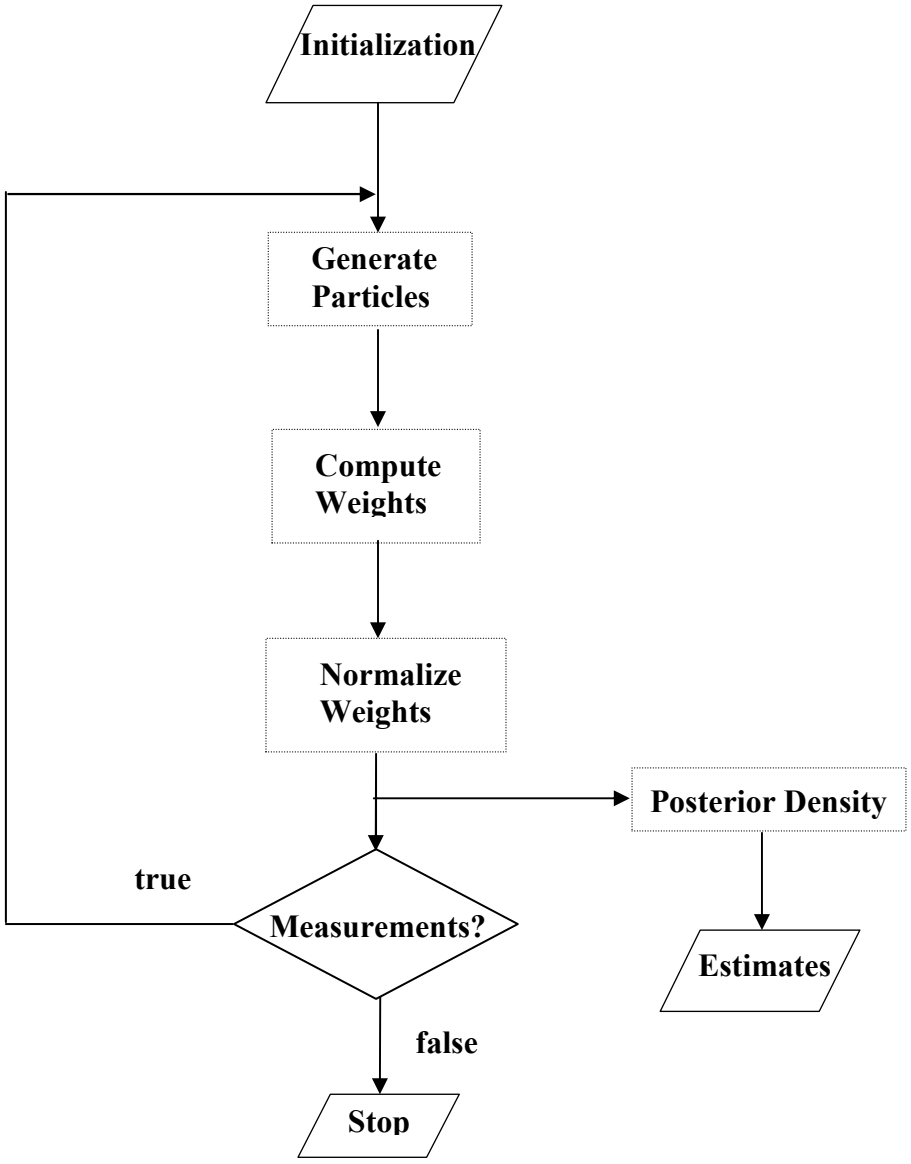

Figure 17 : Flow chart for Sequential Importance Sampling Algorithm

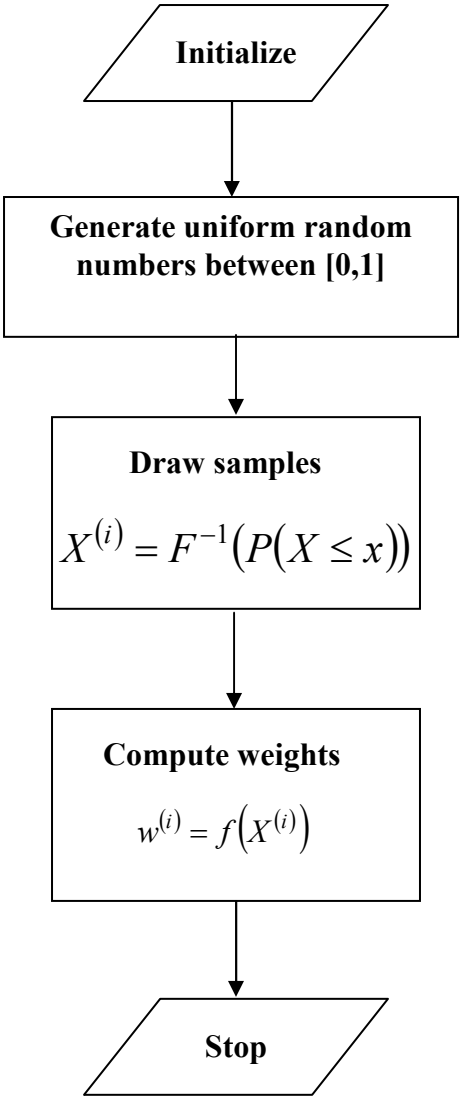

Figure 18 : Flow chart for drawing random samples from a standard probability distribution

5.3 Sampling Importance Resampling Algorithm (SIR)

One of the problems associated with Sequential Importance Sampling algorithm is degeneracy of the particles as the number of iterations increase. Due to this phenomenon, all but a few particles will have a negligible weight. So, large amount of computation has to be expended on particles which will have negligible contribution in the posterior density function. Because of degeneracy, the posterior density is represented by a few particles based on which if estimates are computed does not guarantee accuracy as well the confidence in estimate. In order to overcome the problem of degeneracy, re-sampling methods have been proposed which can be introduced after the normalization step in SIS algorithm. Resampling avoids the degeneracy by selectively sampling the particles based on weights computed in the normalization step. The basic idea used in resampling is to replicate the particles with high normalized weights and eliminate the ones with lesser weights such that the posterior density is concentrated densely in the areas where probability will be high and sparsely where it is low. Figure 19 illustrates the technique of resampling.

A suitable measure of degeneracy is the effective sample size denoted as N_{eff} . Resampling introduces additional computational cost to the SIS algorithm and hence can be applied whenever degeneracy is below the threshold say $N_T = \frac{N_S}{3}$. A variant of SIS with resampling is called Sampling Importance Resampling (SIR) algorithm where

resampling is performed in every iteration. Flow chart for SIR algorithm is given in figure 20.

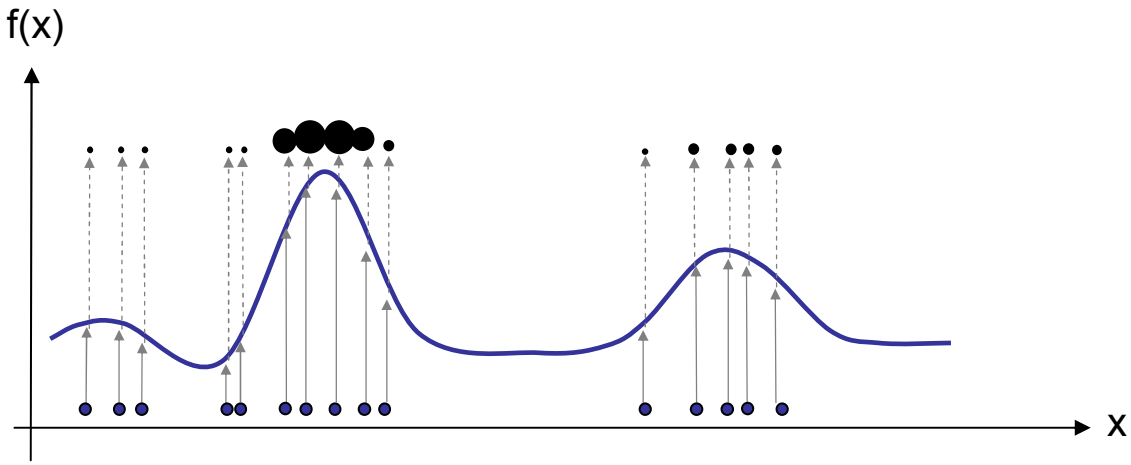

Figure 19 : Resampling Illustration

5.3.1 Pseudo Code for SIR Algorithm

1. Initialize by sampling particles from $P(X_0 \mid Z_0)$ at $k = 0$
2. Iterate steps 3 to 6 for every k
3. Draw samples at k using proposal density $P(X_k \mid X_{k-1})$
4. Compute weights $\tilde{w}_k = P(Z_k \mid X_k)$
5. Normalize particle weights as $w_k{}^i = \dfrac{\tilde{w}_k{}^i}{\sum_{i=1}^{Ns} \tilde{w}_k{}^i}$
6. Resample weights

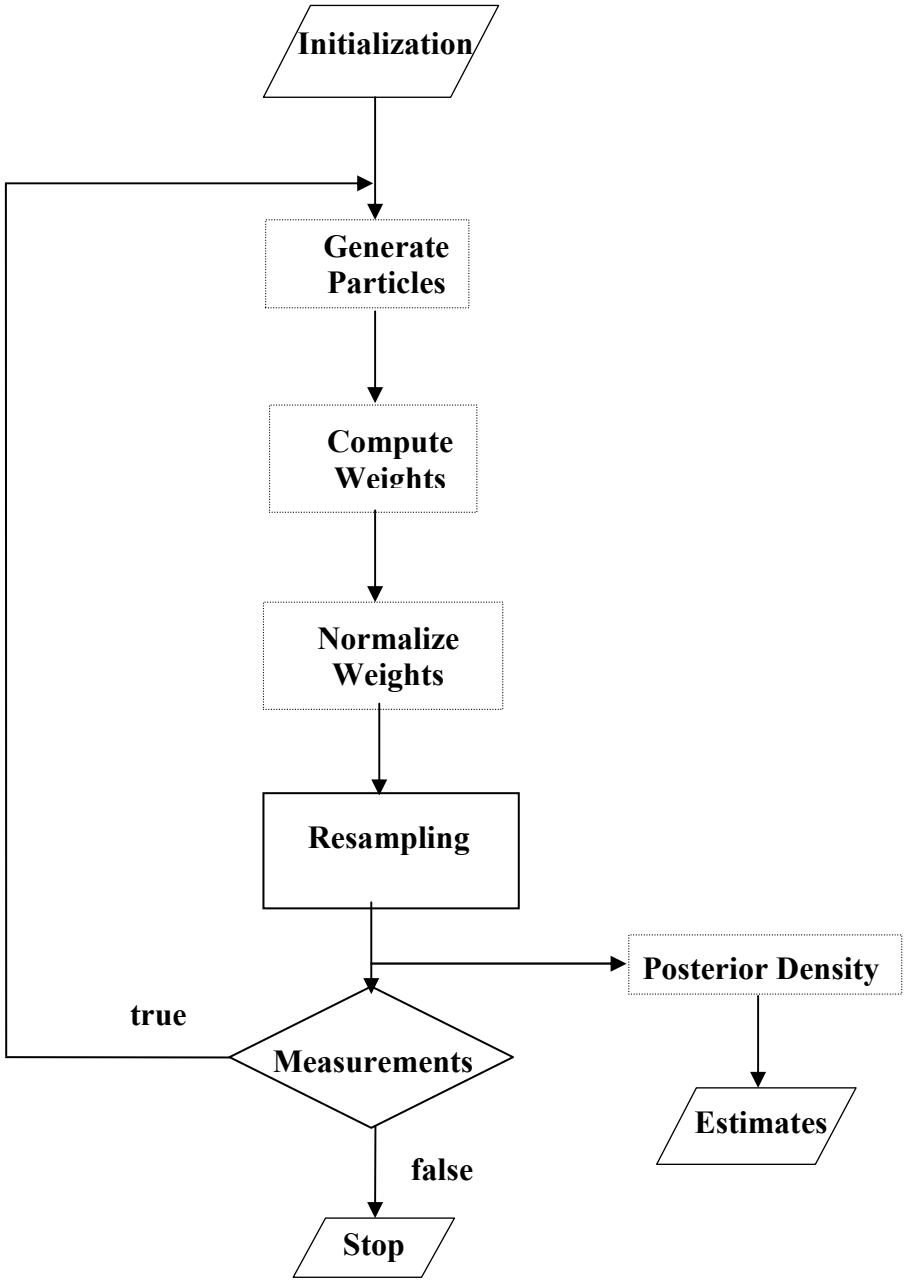

Figure 20 : Flow chart for Sampling Importance Re-sampling Algorithm

One of the disadvantages associated with introducing resampling technique is loss of diversity known as 'sample impoverishment', because of the elimination of particles with lesser probability and replication of particles with higher weights. Also correlation between the particles increases after few iterations, which is not desirable for computing the Monte Carlo estimates. This problem will be more severe when the process noise is small and can be eliminated by introducing Markov Chain moves. MCMC methods can be implemented using any of the algorithms like Metropolis-Hastings, Gibbs sampling and has to be performed whenever the posterior density is resampled. One need not have to worry about burn-in period while implementing Markov chain moves in this scenario, as the weights are an approximation of posterior density and few moves would make the distribution stationary. One drawback of Markov Chain moves is the added computational cost to already computationally expensive Monte Carlo methods. Alternatively, Rao-Blackwell estimator can also be explored by separating the linear and nonlinear parts in the model.

5.4 Simulation Results

This section provides the simulated results of particle filter using SIR algorithm for localization. The initial distribution is assumed to be Uniform in [0,50] for three coordinates. Using the same system parameters as that used for Extended Kalman filter, the particle filter has been simulated with a size of 10000 particles for 100 iterations with a single measurement location. Figure 21 depicts the distribution of particles by means of

a scatter plot which is as expected is a circle in two dimensional plane assuming no fading. Similarly, figure 22 depicts the distribution of particles for a fading channel which are more widely scattered than that in the earlier case.

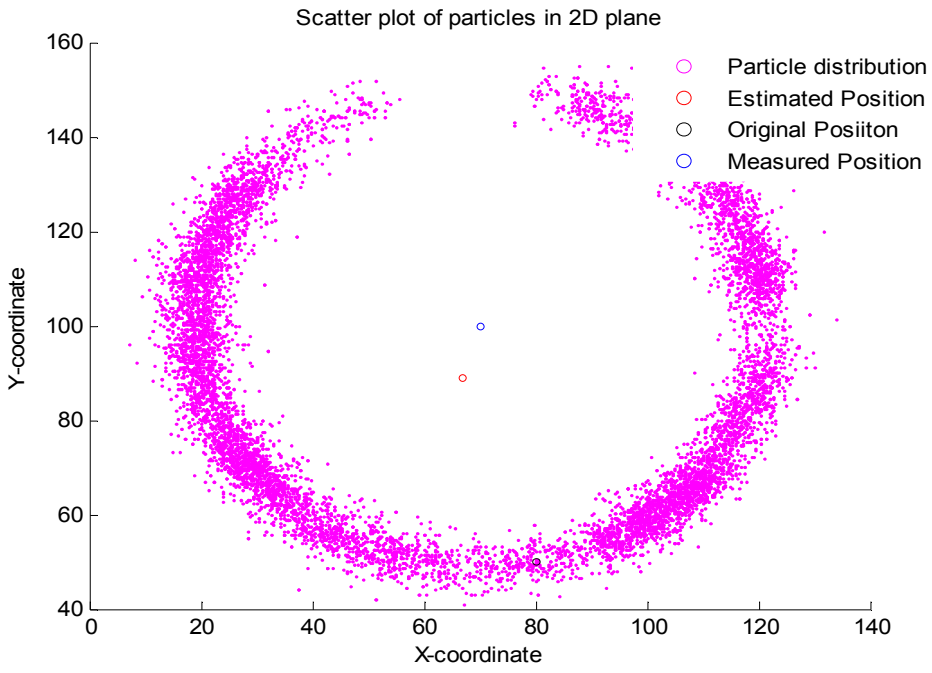

Figure 21 : Distribution of particles for non-fading channel

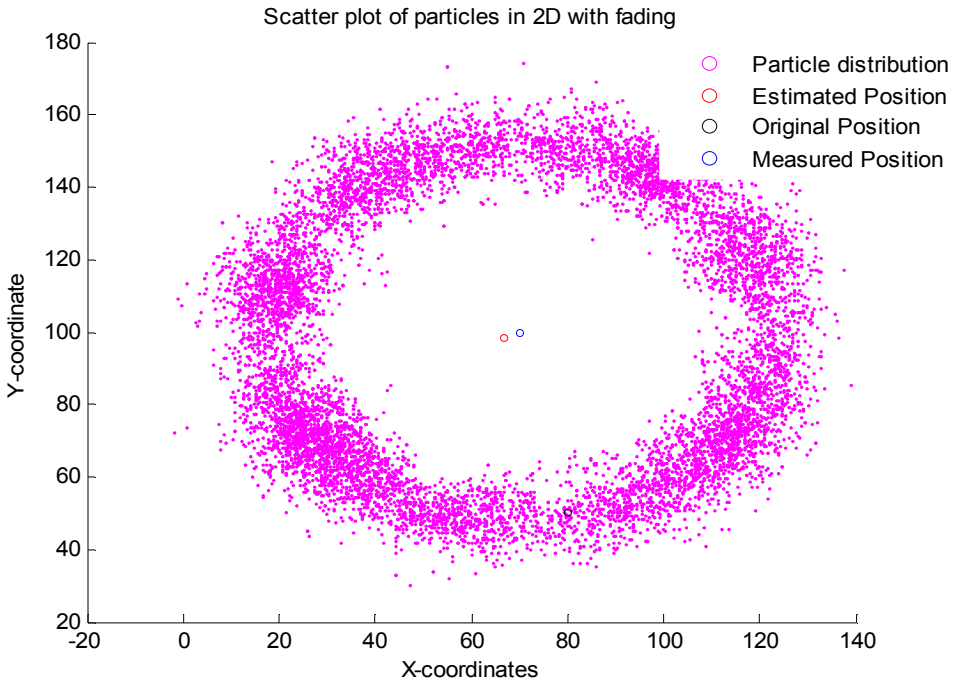

Figure 22 : Distribution of particles for a fading channel

Distribution of particles in the above figures although give some insight about the location of target, they are not useful as the probable region is large. In order to narrow the probable region, measurements are to be performed at multiple locations which when simulated gives the following results depicted in figures 23 - 26. The number of measured locations is chosen to be 25, which provides sufficient accuracy in a two dimensional coordinate system.

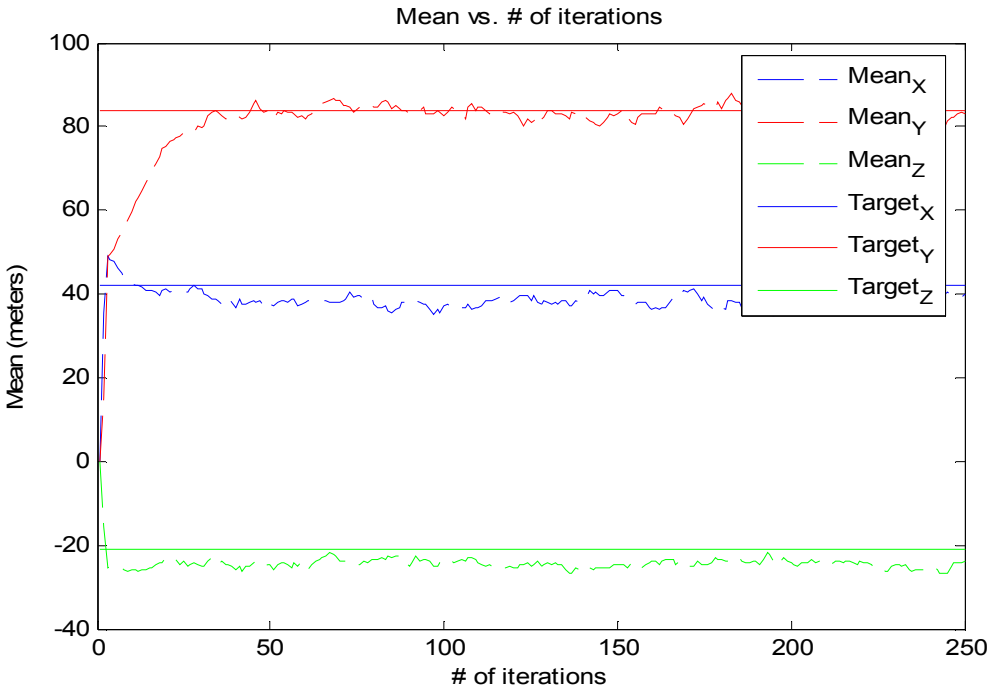

Figure 23 : Mean of the coordinates vs. Time (SIR-PF)

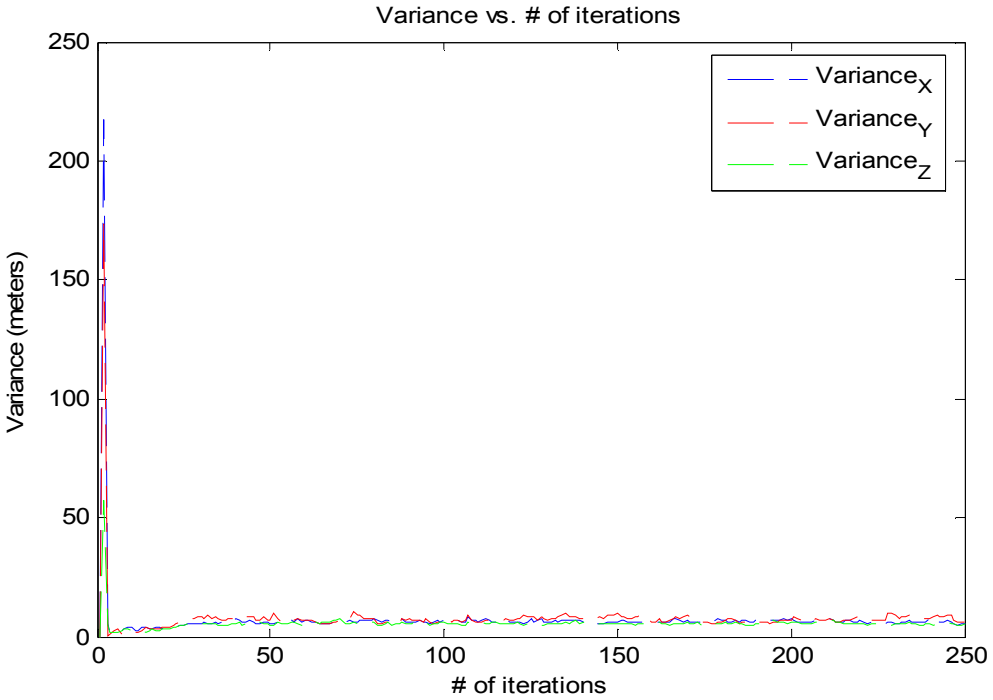

Figure 24 : Variance of the coordinates vs. Number of iterations (SIR-PF)

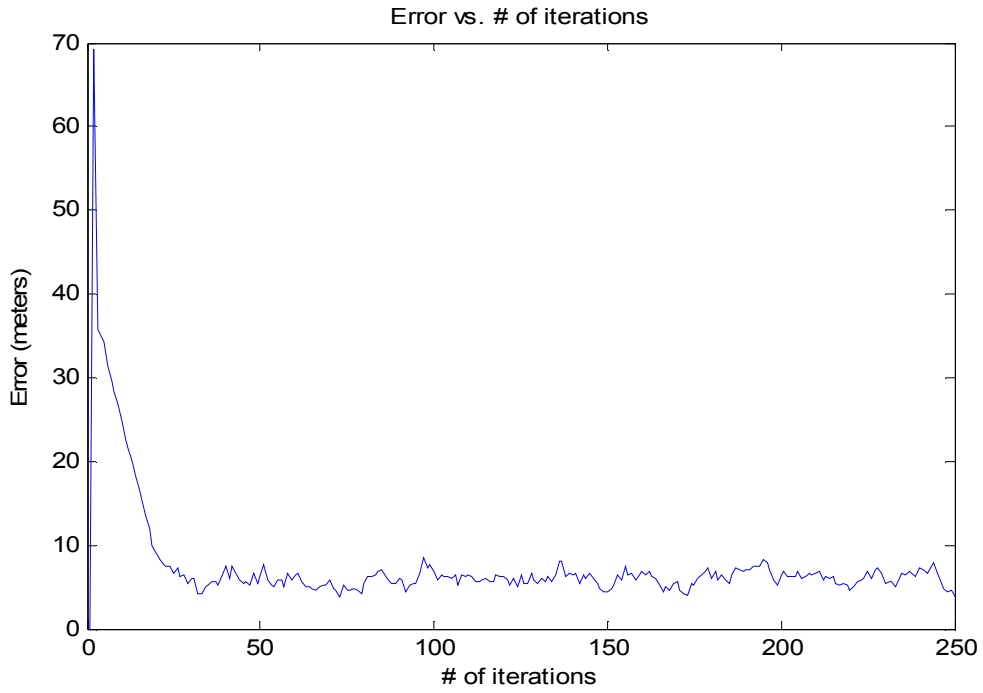

Figure 25 : SIR-PF Error vs. Number of iterations

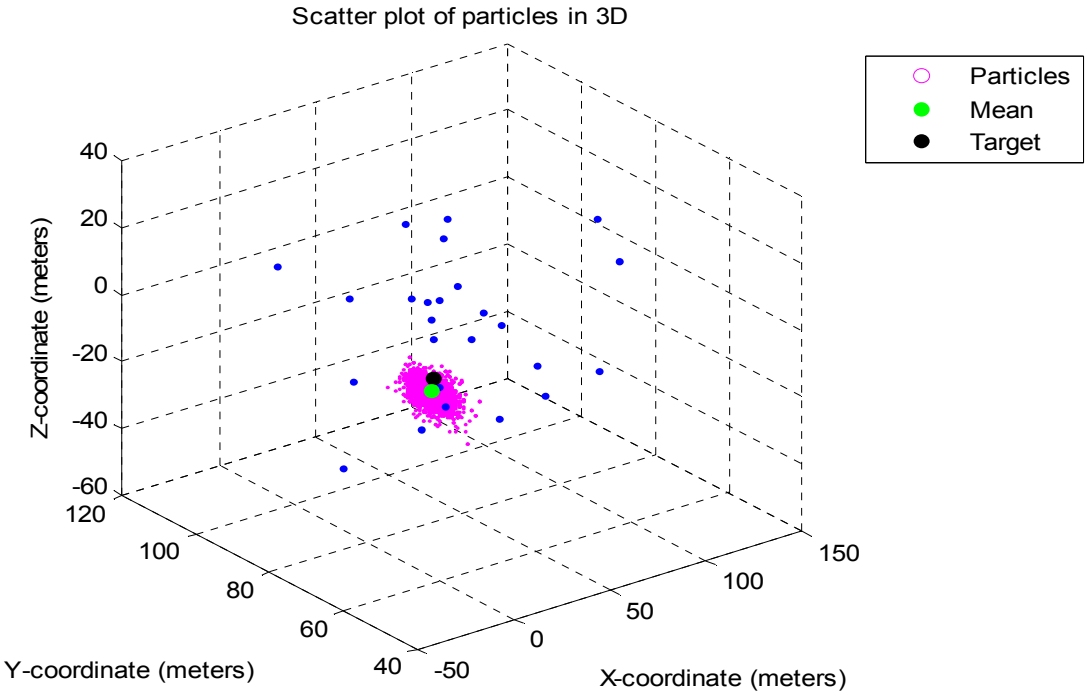

Figure 26 : SIR-PF Scatter plot for distribution of particles

6. COMPARISON, CONCLUSIONS AND FUTURE SCOPE

In the previous chapters we studied the techniques of Least squared error, Extended Kalman filtering and Particle filtering with Sampling Importance Resampling algorithms for localization. This chapter presents the comparison results of the three algorithms, conclusions and the future work.

6.1 Comparison of RLSF, EKF and SIR-PF

Figure 27 provides the simulation result comparing the performance of RLSF, EKF and SIR-PF with mean and maximum likelihood estimates. As observed from chapter 4 simulation, EKF provides better results than RLSF, and from the below figure it can be inferred that SIRPF also performs better than RLSF. Performance of SIR-PF is observed to be comparable to that of EKF, and in this application it in fact provided better results. This is because of the less number of particles (5000) iterated for 250 times for obtaining simulation results; and can be overcome by increasing particle count and/or iteration time. But, the computation time required will also increase and hence a trade off has been made between accuracy and computation time.

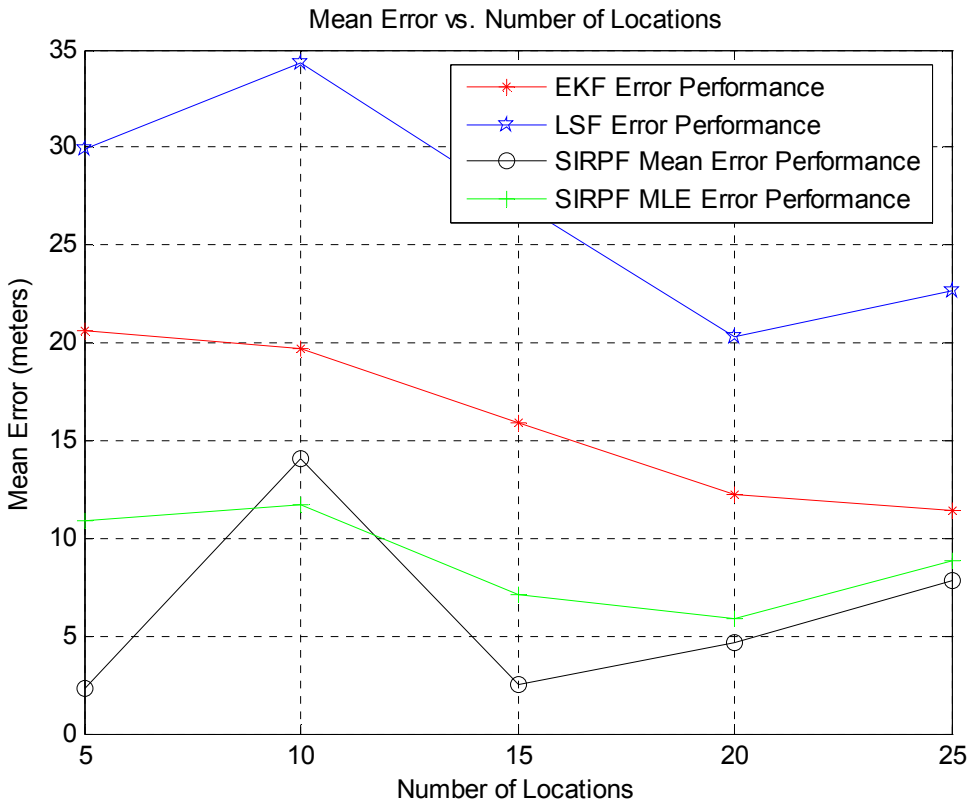

Figure 27 : Comparison of RLSF, EKF and SIR-PF error performance

6.2 Conclusions and Future Work

In this work, three different approaches have been analyzed for localization and their performances are compared. Solution obtained using RLSF minimizes the squared error with obtained measurements but does not provide any statistical information about target location. Whereas the other two solutions EKF and SIR-PF aim to derive the probability density of target location conditioned on the measurements using Bayesian Estimation. Solution obtained using these techniques are considered to be complete as it embeds all the statistical information of system states. As the state space model is found to be nonlinear for this particular application, optimal solution does not have closed form

solution and hence approximations have to be applied. EKF approximates the nonlinear model with a linear one, using Taylor's series expansion and also assumes that the state posterior density is Gaussian. SIR-PF approximates the probability density with weighted particles which are applied to recursive steps of prediction and update to derive the state posterior density. The solution obtained using SIR-PF is preferred to other two techniques because of its generalized approach with out any restrictions on the model or the distribution of state vector. Simulation results also confirm that SIR-PF performance is superior compared to the other two solutions.

For particle filters, it is desired that proposal density closely approximates the posterior density in order to get better estimates with minimum variance. In SIR particle filter, prior density is used as the importance density which does not take in to account the current measurement and hence the samples are drawn from a wider distribution. On the other hand if particles are sampled from a distribution which is conditioned on the current measurement are most likely to be closer to the true estimate. Auxiliary particle filter introduced in [21], uses a proposal density which generates samples from the previous iteration based on current measurement. Performance of this filter has to be explored as it claims better results for systems with low process noise. Also, techniques for building proposals that approximate the posterior density more closely have to be developed and is the area that has to be explored.

REFERENCES

REFERENCES

[1] Greg Welch and Gary Bishop; "An Introduction to the Kalman Filter", The University of North Carolina at Chapel Hill, TR95-041, July 24, 2006.

[2] Tony Lacey; "Tutorial: The Kalman Filter, 11th Chapter" Course CS7322: Computer Vision-II, Spring 1998, Georgia Institute of Technology.

[3] Thomas Kailath, A.H.Sayeed, and B.Hassibi; "Linear Estimation", 2000 by Prentice Hall, ISBN 0-13-122464-2.

[4] Kalman R.E.; "A New Approach to Linear Filtering and Prediction Problems", Trans. ASME, Journal of Basic Engineering, pp. 35-45, March 1960.

[5] Sanjeev Arulampalam, Simon Maskell, Neil Gordon, and Tim Clapp; "A tutorial on Particle Filters for On-line Non-linear/Non-Gaussian Bayesian Tracking".

[6] J.M.Hammersley, D.C. Handscomb; "Monte Carlo Methods", 1965, Fletcher & Son Ltd, Catalogue No. 12/5234/64.

[7] Eric C. Anderson; "Monte Carlo Methods and Importance Sampling", October 20, 1999, Lecture Notes for Stat 578.

[8] Olivier Cappe, Simon J. Godsill, Eric Moulines; "An Overview of Existing Methods and Recent Advances in Sequential Monte Carlo", Vol. 95, No. 5, May 2007. Proceedings of the IEEE.

[9] Miodrag Bolic; "Theory and Implementation of Particle Filters", 12 Nov, 2004.

[10] Arnaud Doucet, Simon J Godsill, Christopher Andrieu; "On Sequential Monte Carlo Sampling methods for Bayesian Estimation", Statistics and Computing, 2000, pages 197-208.

[11] T.S. Rappaport, J.H Reed, and B.D. Woerner; "Position Location Using Wireless Communications on Highways of the Future". IEEE Communications Magazine, Volume 34, Issue 10, Oct. 1996, Page(s): 33 - 41.

[12] Kiran Yedavalli, Bhaskar Krishnamachari, Sharmila Ravula, and Bhaskar Srinivasan; “Ecolocation: A sequence based technique for RF Localization in Wireless Sensor Networks”, Information Processing in Sensor Networks, 2005, 15 April 2005 Page(s):285 - 292.

[13] R. O. Schmidt, "Multiple Emitter Location and Signal Parameter Estimation", IEEE Trans. Antennas and Propagation, Volume AP-34, Issue 3, Mar. 1996, Page(s): 276- 280.

[14] Arnaud Doucet, Nando de Freitas, and Neil Gordon; “An Introduction to Sequential Monte Carlo Methods”. Sequential Monte Carlo Methods in Practice, eds. Arnaud Doucet, Nando de Freitas and Neil Gordon. 2001.

[15] N. B. Priyantha, A. Chakraborty and H. Bala krishnan; “The Cricket Location-Support System”, In Sixth Proceedings of MOBICOM, New York, August 2000.

[16] Bahl P., Padmanabhan, V. N.; “RADAR: An In-Building RF-Based User Location and Tracking System”. Proc. IEEE Infocom, Volume 2, 26-30 March 2000, Page(s):775-784.

[17] K. Spingarn; “Passive position location estimation using the extended Kalman filter,” IEEE Dunsuctions on Aerospace and Electronic Systems, Volume AES-23, Issue 4, July 1987 Page(s):558 - 567.

[18] Yong-An Zbang, Di Zhou and Guang-Ren Duan; “Passive Position Location Estimation Using Particle Filtering”, 8th international Conference on Control, Automation, Robotics and Vision Kunming, China, Volume 3, 6-9 Dec. 2004, Page(s):1635 – 1639.

[19] Samir Soliman, Parag Agashe, Ivan Fernandez, Alkinos Vayanos, Peter Gaal, and Milan Oljaca; “GPS-one^{Tm}: A Hybrid Position Location System”, Volume 1, 6-8 Sept. 2000 Page(s):330 - 335 vol.1, 2000.

[20] R. Roy and T. Kailath, “ESPRIT-Estimation of signal parameters via rotational invariance techniques,” IEEE Trans. Acousr., Speech, Signal Processing, vol. 37, pp. 984-995, July 1989.

[21] M. Pitt, and N. Shephard, “Filtering via Simulation: Auxiliary Particle Filters”. Journal of the American Statistical Association, 1999, Volume 94(446). pp.590-599.

CURRICULUM VITAE

Anoop Kumar Palvai graduated from Sir C.V.Raman Junior College, Hyderabad, India, in 2001. He received his Bachelor of Technology from Jawaharlal Nehru Technological University, Hyderabad, India, in 2005. He secured a score of 95.70 percentile in Graduate Aptitude Test in Engineering, conducted by Indian Institute of Technology – Bombay, India, in 2005. He worked as Graduate Research Assistant at Communications and Networking Laboratory, George Mason University, Fairfax, Virginia. His research interests are in the field of Wireless Communications, Digital Signal Processing and Detection Estimation Theory.